Consolidation and Stabilization

Condition, Conservation, and Reinforcement of the Yumen Pass and Hecang Earthen Ruins near Dunhuang

Wang Xudong, Li Zuixiong, and Zhang Lu

Abstract: *The ancient Yumen (Jade Gate) Pass, located about 90 kilometers northwest of Dunhuang, on the bank of the Shule River in the Gobi Desert, was established in the Western Han dynasty and was a vital gateway on the northern route of the Silk Road. The Hecang Fortress, 11 kilometers northeast of the Jade Gate, also dates from the Western Han dynasty. Both sites, constructed of earth, have been preserved in the arid environment, but after more than two thousand years of exposure they are severely deteriorated. Conservation and consolidation were urgently needed. Investigation of the condition of the sites, together with physical, chemical, and mechanical tests of their earthen material, revealed two categories of problems: weathering of walls and foundations and cracking and collapse of walls. Potassium silicate solution and antiweathering techniques were used to consolidate the most severely weathered walls, and foundations were buttressed with adobe bricks. Cracked walls were reinforced by grouting and bolting, and collapsed walls were restored with rammed earth. These measures are in line with conservation principles for site preservation and are an important experiment in the conservation of earthen structures, affording successful examples for the preservation of similar structures in the region.*

The ruin of Yumen Pass, also called Xiaofangpan Fortress, is located on the Shule River in the Gobi Desert approximately 90 kilometers northwest of Dunhuang (fig. 1). Built during the Western Han dynasty, it served as a strategic point on the northern Silk Road and played an important role in the development of the Western Regions (Compiling Committee 1996). The extant structure is a square fortress with an area of approximately 702 square meters (26.4 m by 26.6 m). The

FIGURE 1 Condition of the Yumen Pass before consolidation.

walls, approximately 10 meters high, were built of rammed earth (fig. 2).

Hecang Fortress, also known as Big Fangpan Fortress, is on a tableland on the south bank of the Shule River, 11 kilometers northeast of the Yumen Pass (fig. 3). It too was built during the Western Han dynasty, and it was rebuilt during the Western Jin dynasty. Li Zhengyu (1996: 302–3) believes that it was originally the Chang'an granary for the Dunhuang prefecture in the Han and Jin periods. It is in the form of a square with collapsed walls. In the north there is a 2-meter-high natural platform extending from east to west, on which a rectangular granary (132 m by 17 m) was constructed with three spacious rooms. All rooms face south. The roof collapsed long ago, and it is impossible to know what it was like. The southern wall and a partitioning wall have mostly collapsed. The other three walls and the other partitioning walls
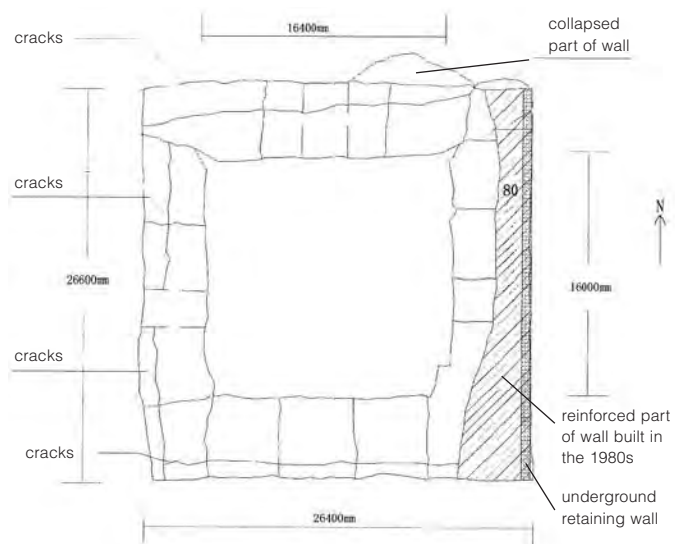
351

FIGURE 2 Layout of the Yumen Pass.

FIGURE 3 Condition of the Hecang Fortress before consolidation.

have survived. These walls have an average height of 6 meters and a thickness of 1.5 meters. In the upper and lower parts of the walls there are two rows of evenly distributed triangular ventilating holes. Of the walls encircling the granary, only the eastern, northern, and western ones have their foundations partially preserved. Of the four corner towers, only the southwestern one is extant; the other three have only their foundations preserved.
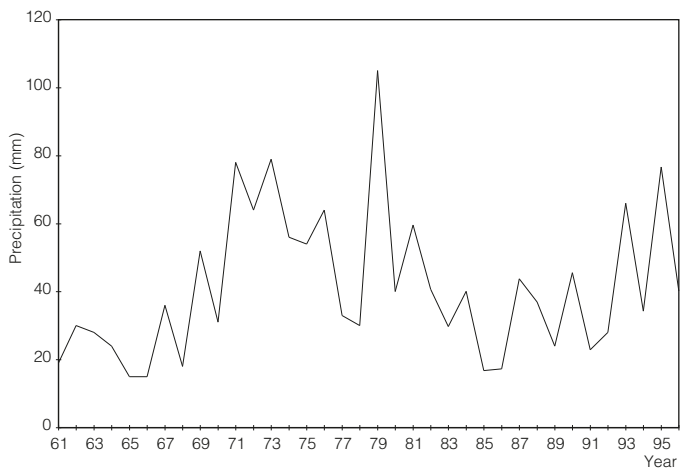

FIGURE 4 Yearly precipitation in the Dunhuang area.

Earthen structures of the Western Han dynasty are now rare. They bear significant value for an understanding of the history, agriculture, communication, military affairs, and architecture of the Western Han and Western Jin dynasties.

The Yumen Pass and Hecang Fortress were able to survive due to the arid climate, but recent investigation showed that immediate conservation was needed to prevent further deterioration. With this vision, we conducted intramural and field tests (Li Zuixiong, Zhang H., and Wang Xudong 1995; Su Bomin, Li Zuixiong, and Hu Z. 2000; Li Zuixiong, Wang Xudong, and Tian L. 1997; Li Zuixiong and Wang Xudong 1997). These tests were evaluated and approved by the State Administration of Cultural Heritage before implementation.

Local Climate

Precipitation

Temperature and rainfall are two factors that affect the earthen structures. As shown in figure 4, annual precipitation in the Dunhuang area between 1961 and 1996 was characterized by extreme instability. Meteorological records kept at the Dunhuang station show that 1979 and 1956 mark the two extremes, 105.5 millimeters and 6.4 millimeters, respectively. The annual precipitation is in general on the increase. The evaporation volume, however, is stable and falls between 2,200 and 2,700 millimeters.
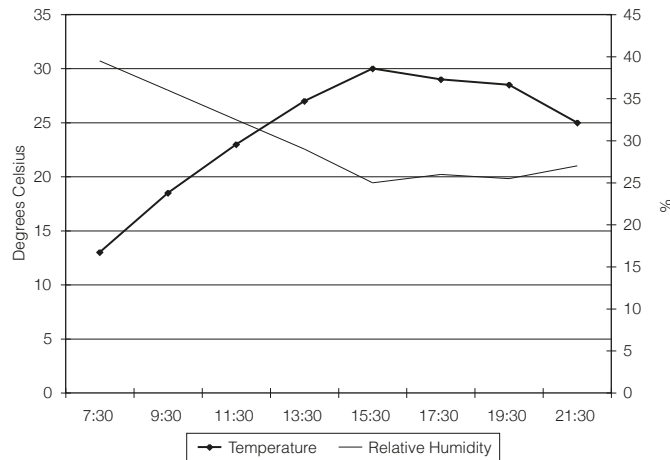
FIGURE 5 Humidity variations on August 27 at the Hecang Fortress.

Temperature and Humidity

A preliminary recording of temperature and humidity was undertaken from August 21 to September 25, 2000, at the Hecang Fortress during our consolidation operations. Data were recorded every two hours between 7:30 and 21:30 from a thermohydrograph placed in the shade. Although these data do not cover twenty-four hours, they reflect the regularities of temperature and humidity fluctuations during this period and served as useful information for the conservation work.

During this period, daily mean temperature showed a declining trend, while the daily mean humidity rose slightly. For example, as shown in figure 5, on August 27 temperature rose from the lowest point at 7:30 to a high between 13:30 and 15:30 and thereafter began to drop. The relative humidity declined from the highest value at 7:30 to the lowest point between 13:30 and 15:30 and thereafter began a slow rise. The daily temperature fluctuation was large, with a maximum of 19.5°C, a minimum of 10.5°C, and an average difference of 14.96°C. The daily humidity change was also considerable. In sum, temperature at the Hecang Fortress was relatively high, with a wide fluctuation range, and humidity was low.

The best temperature range for potassium silicate (PS) solution infiltration is between 18°C and 25°C, and the acceptable working temperature range is 15 to 30°C (Li Zhengyu 1996). Adjustment can be made on-site if needed, so that the optimal effect of PS reinforcement can be attained.

Properties of the Earth

Yumen Pass

Table 1 gives the physical properties of the earth from the Yumen Pass, and table 2 shows the analysis of the soluble salts. The soluble salts are mainly chloride and sulfate—NaCl, $CaSO_4$, $MgSO_4$, with pH values of 7.39–8.50—and the earth is alkaline. The total salt content is higher in the upper

Table 1 Physicodynamic Properties of the Earth from Yumen Pass

		Middle, North Wall West	Upper Part, North Wall West	Lower Part, North Wall West	Bottom, North Wall West	Massive Sample
Moisture content (%)		1.3	1.1	1.7	1.6	2.9
Dry density (g/cm³)						1.87
Porosity ratio						0.480
Saturation (%)						16.3
Porosity rate (%)						32.4
Soil grain gravity		2.70	2.69	2.69	2.69	2.69
Liquid limit (%)		25.6	20.4	22.8	24.3	23.6
Plastic limit (%)		16.2	13.8	16.1	16.8	16.5
Plasticity index		9.4	6.6	6.7	7.5	7.1
Particle size	0.25–0.075 mm		16.5%	13.5%		8.5%
	0.075–0.005 mm		72.5%	72.5%		77.5%
	0.005 mm		11.0%	14.0%		14.0%

Table 2   Soluble Salts in the Earth from Yumen Pass

Wt% / Sample Location	Bottom, North Wall West	Lower Part, North Wall West	Middle, North Wall West	Upper Part, North Wall West
CO_3^{2-}	0.001			
HCO_3^-	0.018	0.028	0.022	0.019
Cl^-	4.861	0.166	0.098	0.020
SO_4^{2-}	1.195	0.130	0.205	0.454
Ca^{2+}	0.026	0.009	0.061	0.139
Mg^{2+}	0.005	0.001	0.004	0.005
$Na^+ + K^+$	3.767	0.185	0.101	0.075
pH	7.39	8.50	7.98	8.04
Total salt content (Wt%)	9.995	0.519	0.477	0.735

Table 3   Physical Indices of the Soil at Hecang Fortress Ruins

Sample Location	Pedestal, SW Corner	Pedestal, NW Corner	Pedestal, NE Corner	Pedestal, SE Corner	West Wall	North Wall
Density (g/cm³)	1.838	1.915	1.643	1.923	1.897	1.762
Porosity ratio	0.476	0.411	0.658	0.472	0.426	0.554
Porosity rate (%)	32.18	29.08	39.60	31.75	29.76	35.46
Particle gravity	2.71	2.70	2.72	2.71	2.70	2.73
Liquid limit (%)	25.2	21.4	32.3	23.1	22.3	32.2
Plastic limit (%)	14.1	14.6	18.7	11.2	14.0	16.6
Plasticity index	11.1	6.8	13.6	11.9	8.3	15.6
Particle size — 0.25–0.075 mm	21.23	23.93	4.85	61.47	27.93	28.58
Particle size — 0.075–0.005 mm	66.33	72.81	82.65	31.81	68.74	60.65
Particle size — 0.005 mm	12.44	3.26	12.50	6.72	3.33	10.77
Particle size — d_{10}	0.0031	0.0282	0.0036	0.0086	0.0273	0.0046
Particle size — d_{30}	0.0212	0.039	0.0175	0.0276	0.0333	0.0243
Particle size — d_{60}	0.055	0.049	0.0535	0.113	0.0416	0.0605
Soil classification	silt	silt	silt	silt	silt	silt

part of the walls than in the middle and extremely high at the bottom. This is the result of a high rate of evaporation and capillarity from the ground.

Hecang Fortress

Table 3 shows the physical properties of the earth from the Hecang Fortress. It can be seen that the density of the earth samples is irregular, which is a characteristic of artificial earth structure. Due to the different extents of weathering, uneven particle sizes, and partial calcareous nodules, the samples vary widely in density and porosity. The greater the dry density, the less the porosity and the more solid the earth.

Because of the partial calcareous nodules or sand lenticles, as well as evident differences in the particle size, the difference in the speed of disintegration on wetting varied greatly: from rapid (17.46 g/min) to slow (less than 0.1 g/min). On the whole, nonuniform engineering performance

might result from uneven soil density so that the strength and stability might be adversely affected.

Chief Problems of the Yumen Pass and Hecang Fortress

Weathering of Walls and Foundations

There are two types of weathering: chemical and physical. Chemical weathering results from enrichment of soluble salts in the wall foundations. Because of precipitation and capillarity, soluble salts dissolve, crystallize, and dissolve again and finally lead to the destruction of cohesive forces and the erosion of wall and foundations. Physical weathering is erosion by wind and rain. It is windy in the Dunhuang area throughout the year, causing the formation of honeycomb on the surface of walls. Although precipitation is generally low, when heavy it contributes significantly to erosion, as it softens and disintegrates the earth. High evaporation following heavy rain quickly dries and turns the softened wall surface into scalelike crusts, which fall off under the combined forces of wind and rain.

Cracking and Collapse of Walls

The weathering described above bites into wall foundations and changes the stress distribution of the wall body, which causes cracks parallel to the wall surface. Cracks are normally 2 to 5 centimeters wide, but they can be up to 10 centimeters wide. This is worsened by fissures left by the ramming operations when the walls were built. So when it rains or an earthquake occurs, the walls easily collapse. Collapse may

also happen along the fissures between ramming layers, as the fissures grow under natural forces.

Conservation

Foundation Reinforcement

Where wall foundations were eroded, the surface was cleaned of friable earth. PS solution was infiltrated into the area to consolidate it; thereafter, adobe bricks with a dry density of no less than 1.75 grams per cubic centimer were laid to support the foundation. Surface treatment was done for visual compatibility. Figures 6 and 7 show an area of the Hecang Fortress before and after reinforcement.

Surface Consolidation

PS solution with a lower concentration (generally 2 to 3 percent) was used to harden the surface of walls exposed to intense wind and rain. The solution was injected into the target areas repeatedly. In the case of scaling wall surface, PS-C solution was used to bind the scales to the wall body. After drying, mud with PS solution was applied so as to restore the original appearance of the wall.

Potassium silicate was the primary material for reinforcing the walls and foundations of the Hecang Fortress. After the softened areas were cleaned, three PS solutions of varying concentrations were sprayed on them at intervals of a week to ensure complete infiltration: 2 to 3 percent solution the first time, 5 percent solution the second time, and 7 percent solution the third time. Ten percent PS solution with added earth was applied to the softer and more porous

FIGURE 6 Hecang Fortress before consolidation.

FIGURE 7 Hecang Fortress after consolidation.

areas to cement large grains of clay. Finally, mud from local earth was used to restore the original look.

Multiple applications of low-concentration PS solutions are important in the treatment strategy for conserving earthen structures (Li Zuixiong, Zhang H., and Wang Xudong 1995). It maximizes deep infiltration and minimizes the concentration gradient so that the treated surface will not be too strong to hold to the wall. So far this strategy has been effective.

Reinforcement of Cracked Walls

Anchor Rod Reinforcement at Yumen Pass. Unlike the traditional method of support, which aims to hold back the collapsing rock or earth, an anchor rod strengthens the body of rock or earthen structure itself, effectively preventing it from deforming and collapsing. It is also advantageous in that it does not jeopardize the appearance of a treated structure.

The anchor rods used are hot-rolled iron bars, and the binding materials are cement mortar; we have also studied binding materials suitable for anchoring and selected PS-F, PS-C, and others (Li Zuixiong, Wang Xudong, and Tian L. 1997). Anchor washers, made of iron plates, were used to hold the target area (Liang J. 1999). They were secured only with bolts and caps onto the anchor rods (fig. 8).

This anchoring system was used to reinforce the northern, western, and southern walls of the Yumen Fortress. Holes were typically drilled at an interval of 1.5 meters vertically and 1.0 meter horizontally. Their depths varied but in general exceeded 1.0 meter. Lower rows of holes were drilled at an angle of 10 to 15 degrees; the upper rows of holes were drilled at a smaller angle or horizontally. All the holes were 50 millimeters in diameter. In order to reduce vibration, drilling was done manually. Rods were 45-millimeter-diameter iron pipes with wooden sticks inside and corrosion-proof mate-

rials coating the outside. PS solution was poured into the holes to pretreat the walls of the holes, PS and clay solution or PS-F liquid was poured into them, and finally the anchor rods were inserted. A total of 81, 100, 84, 29, and 8 rods were installed in the northern, western, and southern walls and the western and northern gates, respectively. The lengths of rods were determined on the spot and varied from 0.50 meter to 4.50 meters.
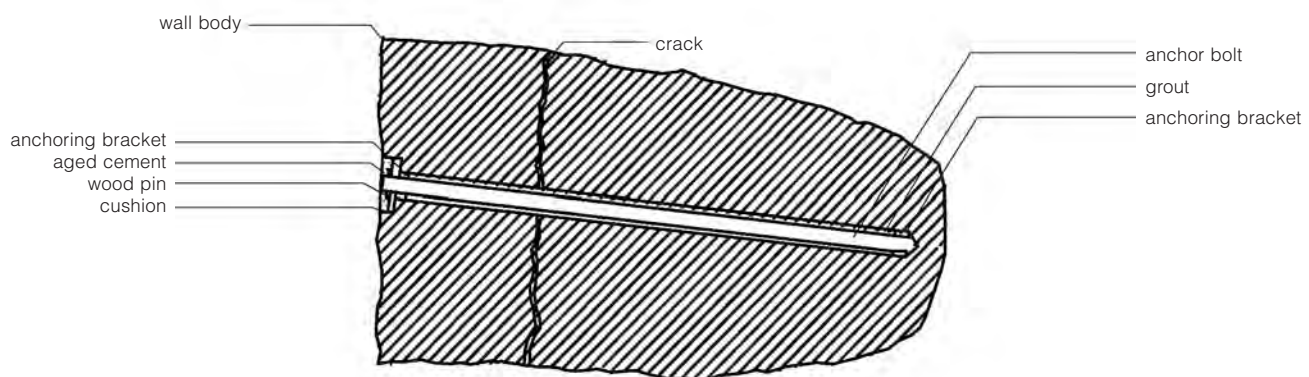
Grouting and Draining. Extensive cracks had developed in the walls and gates of the Yumen Pass, and if left untreated rainwater would seep into the cracks, weaken the walls, and eventually lead to collapse. Cracks were filled with earth, and PS-F or PS-C solution was added so as to consolidate them. Also, drainage was installed to remove rainwater.

Reinforcement of Collapsed Walls

North Wall of the Yumen Pass. The north wall of the Yumen Pass had partially collapsed. To secure the extant portion, a new rammed wall was built in collapsed areas and integrated with the old wall with "soil nails" and reinforced earth. Soil nailing is a technique that consolidates an earthen surface by nailing steel netting into the surface and coating the nails and nets with cement (Cheng Liangkui, Zhang Z., and Yang Z. 1994). This technique has been widely used in quarrying works (Zeng Xianming, Huang J., and Wang Z. 2000), but its use in cultural property conservation is rare.

These techniques were employed in reinforcing the collapsed northern wall of the Yumen Pass. Local earth was also used for making new rammed earth walls. Earth was crushed and soaked before being mixed with lime. This mixed earth was then used for forming new wall. Layers ~18 centimeters thick were laid and rammed manually until reduced to 15 centimeters. Reinforcing iron frames, 300 by 300 millimeters, were placed both horizontally and vertically in the

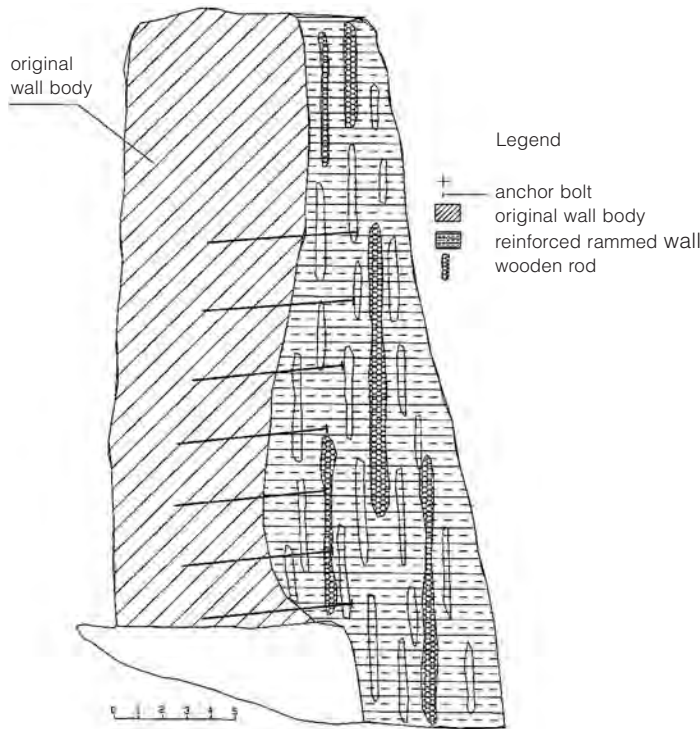**FIGURE 8** Section view of anchor rod structure.

FIGURE 9 Soil mass consolidated with *Achnatherum* stalks on the northern wall.

rammed earth. *Achnatherum* stalks were laid crosswise on each layer to increase the bonding strength of the new wall. PS-tempered clay was used to fill the fissure between the new and old walls (fig. 9).

East Wall of the Yumen Pass. A brick wall foundation (25 m long, 0.5 m wide, and 40 cm deep) was laid along the footing of the reinforcing wall built in the 1980s to prevent the wall from sliding. The original wall was consolidated with PS solution. Along the original wall, a

FIGURE 10 Reinforced outer section of the northern wall.

40~500-centimeter-wide reinforcing wall was built to buttress the original wall.

Conclusion

The Yumen Pass and the Hecang Fortress have survived in the arid environment in northwestern China. Over the past two thousand years, they have suffered cracking, collapse, and wind erosion. Reinforcement work was undertaken to preserve their high historic, scientific, and archaeological values. After a detailed investigation, anchoring techniques were used to consolidate the weathered walls with potassium silicate materials. Soil nailing and reinforced soil techniques were also used under collapsing walls, and mud bricks were inserted to support walls and the platform (fig. 10). These measures guarantee the preservation of these unique earthen structures while complying with the principles of cultural property conservation. It is also a valuable trial of rock and soil reinforcement techniques in conservation and will provide examples for conserving earthen structures in northwestern China.

References

Cheng Liangkui, Zhang Z., and Yang Z. 1994. *Practical Techniques of Rock and Soil Reinforcement.* Bejing: Seismology Publishers.

Compiling Committee for the Annals of Dunhuang City. 1996. *Annals of Dunhuang City.* Beijing: Xinhua Publishing House.

Liang J., ed. 1999. *Manual of Anchoring and Injection Techniques.* Beijing: China Electric Power Publishers.

Li Zhengyu. 1996. *A New Perspective of Dunhuang History and Geography.* Taipei: Xinwenfeng Publishing.

Li Zuixiong. 1996. Issues of stability and strength in reinforcing earthen and rock cultural sites. *Dunhuang Studies* 3: 96–106.

Li Zuixiong and Wang Xudong. 1997. Progress in conservation and reinforcement of ancient earthen structures. *Dunhuang Studies* 4: 167–72.

Li Zuixiong, Wang Xudong, and Tian L. 1997. Experimental reinforcement of earthen structures in ancient Jiaohe city. *Dunhuang Studies* 3: 171–81.

Li Zuixiong, Zhang H., and Wang Xudong. 1995. Reinforcement of ancient earthen structures. *Dunhuang Studies* 3: 1–18.

Su Bomin, Li Zuixiong, and Hu Z. 2000. A preliminary study of potassium silicate and its application in earth structure conservation. *Dunhuang Studies* 1: 30–35.

Zeng Xianming, Huang J., and Wang Z. 2000. *Manual of Soil Peg Support and Construction.* Beijing: China Architecture Publishers.

Research and Application Methods for Comprehensive Control of Wind-Borne Sand at the Mogao Grottoes

Wang Wanfu, Wang Tao, Zhang Weimin, Li Zuixiong, Wang Xudong, Zhang Guobing, Qiu Fei, and Du Mingyuan

Abstract: *On the plateau behind the Mogao Grottoes to the west lie megadunes. For centuries wind-borne sand has cascaded over the cliff face, burying the entrances to the caves and accumulating on the elevated walkways of the upper tiers. Some 2,000 cubic meters of sand were removed annually by Dunhuang Academy staff, until the early 1990s, when the 3.7-kilometer-long open-knit wood fence and a windbreak of local xeric plants reduced the quantity of sand by 60 percent. This paper reports on further developments, including new techniques such as straw half buried in a grid pattern, a surface layer of gravel, expansion of the drip-irrigated vegetation fence, and chemical consolidation of sand on the cliff top. Through this multifunctional system that includes engineering, biological, and chemical measures, the objective is to develop comprehensive control of windblown sand.*

The Mogao Grottoes are located in an extremely arid region. On the one hand, dryness and rare rainfall are natural environmental conditions that have favored preservation of the wall paintings in the cave temples. On the other hand, the Mingsha dunes on the plateau above the Mogao Grottoes are an abundant sand source that threatens the site. In recent decades experts have focused on the control of blown sand, and many ideas have been put forth and experiments carried out. The work reported here builds principally on earlier research, testing, and implementation at Mogao on the control of windblown sand by a 3.7-kilometer-long synthetic textile wind fence; the use of desert-adapted plants; and chemical consolidation of sand. This work was published in the proceedings of the International Conference on the Conservation of Grotto Sites, held at Mogao in October 1993 (see Ling Yuquan et al. 1997; Lin et al. 1997; Li Zuixiong, Agnew, and Lin 1997). Engineering protection was discussed by Lin et al. (1997); Qu Jianjun et al. (2001); and Xue Xian, Zhang Weimin, and Wang Tao (2000). A vegetation windbreak and its effects were studied by Wang Wanfu et al. (2004). Meanwhile, the urgency of setting up a comprehensive protection system was discussed by Zhu Junfeng and Zhu Zhenda (1999); Wang Wanfu, Zhang Weimin, and Li Yunhe (2000); Qu Jianjun et al. (2001); Zhang Weimin et al. (2000); and Wang Wenfu et al. (2004).

Through analysis of the effectiveness of drip-irrigated vegetation windbreaks, engineering measures including half-buried straw "checkerboard" barriers, gravel mulch, and nylon fences on the plateau above the Mogao Grottoes, an attempt was made, as described here, to set up a rational, scientifically designed, comprehensive protective system to control windblown sand.

Blown-Sand Environment

The Mingsha sand dunes comprise a 60- to 170-meter-high megadune that is the main source of sand threatening the Mogao Grottoes. Through photographs taken during the same season in 1972 and 1985, using a terrain model, the dune topography was mapped at 1:1000 scale. Qu Jianjun et al. (1997) reported that small dunes at the edge of Mingsha migrate from southwest to northeast. The annual movement of small dunes is 3 to 9 centimeters, with an average of 6 centimeters. The dunes are essentially stable, and small movements at the edges represent little threat to the site. However, the real threats to the site are windblown sand accumulation, wind erosion, and dust storms.
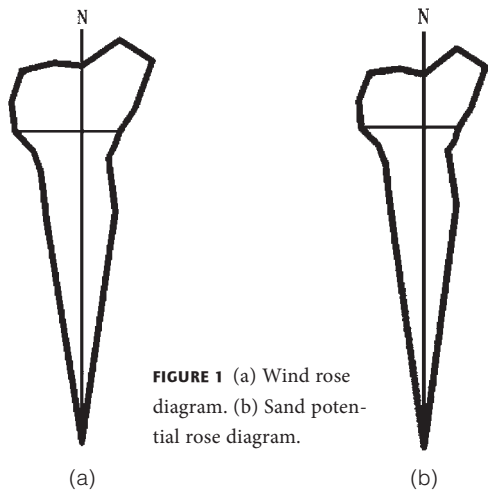
FIGURE 1 (a) Wind rose diagram. (b) Sand potential rose diagram.

(a)   (b)

FIGURE 2 Half-buried straw checkerboard barriers.

Wind data from the meteorological station on the cliff top collected during the period 1990 to 2002 are represented on the wind rose (fig. 1a) and sand-drift potential rose (fig. 1b). Wind rose and sand rose diagrams are based on a polar coordinate system to present their frequency at specific directions. The most common rose diagram has 16 azimuth angles. The length of ray at each azimuth angle is proportionate to the frequency of wind at that specific direction. A sand rose diagram may be different from the associated wind rose diagram because a wind speed of less than 5 ms^{-1} does not carry sand. The drift rose is drawn by a computer program and is based on the quantities of sand collected by a specially designed sand collector with twelve receptacles distributed at 30° to each other. Sand movement results mainly from the westerly and southerly winds, which blow 31 and 30 percent of the time, respectively; the easterly wind blows 15 percent of the time but is weak. The surface material on the plateau comprises gravel, sandy gravel, an area of shifting sand and small dunes, and the megadune, the last being the westernmost. The key to controlling blown sand from the cliff edge is to stabilize and thereby decrease the sand coming from the Mingsha megadune, as described below.

Measures for Controlling Windblown Sand

Straw "Checkerboard" Barriers
The shifting sand is located in an area of small dunes and flat sand sheets at the front edge of the Mingsha megadune. A windbreak fence of open-knit nylon and half-buried straw checkerboard barriers (fig. 2) are the control measures here. The main function of the straw barriers planted in the sand in a square checkerboard grid is to stabilize the shift-

ing sand by changing the roughness of the surface. This decreases the impact threshold velocity, hence the rate of sand transport, and transport from the sand dune field is reduced. This also creates suitable conditions for growth of vegetation. The friction as a result of the straw checkerboard barriers in the areas of shifting sand and small dunes increases thirty to forty times, and the roughness of the surface also greatly increases.

Nylon Wind Fence
Figure 3 shows the plan of the open-knit nylon fence, and figure 4 shows sand accumulation. Over seven years a
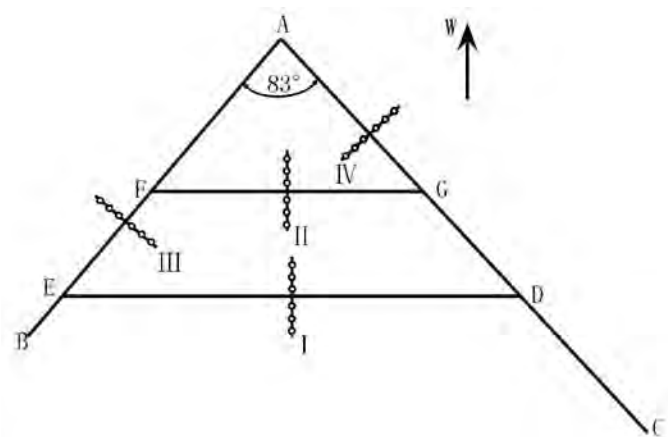

FIGURE 3 Schematic drawing of wind fence and sand depth monitoring sticks along lines I–IV.

FIGURE 4 Sand accumulation around the wind fence.

total volume of 23,000 cubic meters of sand accumulated around the fences. Sand accumulation on the AC segment accounted for 13,000 cubic meters, which shows that the northwest direction is the main source under the control of the westerly winds. Sand accumulation on the AB segment to the southwest accounted for 5,400 cubic meters, which shows that the southwest is another sand source. Sand accumulations on the DE and FG segments were 3,600 and 1,700 cubic meters, respectively, showing sand mainly originating in situ.

Section IV (see fig. 5a) shows that the profiles of sand accumulation under the control of the northwesterly winds vary seasonally and annually. Sand accumulates especially during the windy season, March to July. Sand accumulation in 1992 and 2002 was similar, reaching 30 centimeters.
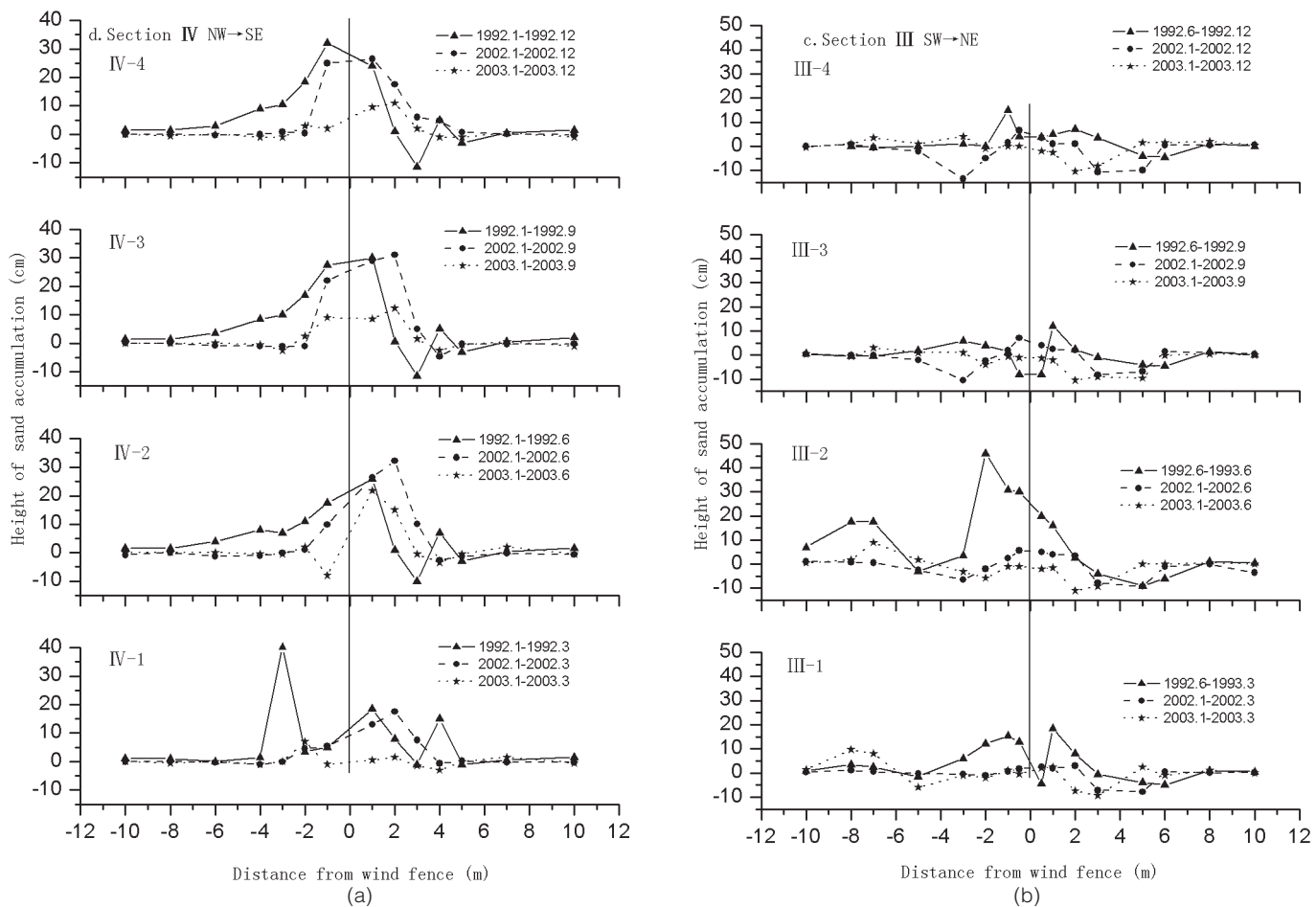

(a)

(b)

FIGURE 5 (a) Section IV sand accumulation on a quarterly basis for the years 1992, 2002, and 2003, showing the upwind and downwind depths. (b) Section III showing sand depths under the influence of the southwesterly wind.

However, after the sand source was further controlled in 2002, the amount of sand around the fence decreased greatly, to about 10 centimeters annually.

Section III (fig. 5b) shows the comparable profiles of sand accumulation for the southwesterly winds. The processes of sand accumulation are most obvious and reach 25 centimeters during the March–July windy season. Wind erosion also occurs, reaching a depth of 10 centimeters.

Large amounts of sand from the Mingsha megadune are arrested by the nylon fences. Southerly winds caused by local air circulation have a higher frequency and longer duration, but the volume of the sand transported is much lower than that carried by westerly winds, and the transport rate decreases gradually from the Mingsha megadune to the top of the grottoes.

Gravel Layer

Gravel placed on sand (a gravel "mulch") is effectively unerodable and increases the roughness and dissipates wind energy. This results in a decrease in the wind velocity and an increase in shear stress of the airflow near the surface, thus decreasing wind erosion. Gravel straw stubble and increasing cover of vegetation windbreaks effectively restrain wind erosion and are effective approaches to control blown sand. But there is some disagreement on coverage.

Based on wind tunnel experiments (Dong Zhibao, Qu Jianjun, and Liu Xian 2001), regardless of the size of the pebbles on a natural gobi surface as long as they cover about 40 to 50 percent of the area, there is no potential sand movement. But according to a study of sand control (Xue Xian, Zhang Weimin, and Li Yunhe 2000), in order to completely eliminate sand erosion of the ground surface at the plateau above the grottoes, more than 65 percent of the area should be covered with pebbles. Field observations showed that sand coming from the Mingsha megadune can be transported to the gravel area when wind velocity is less than 10 ms^{-1}. Because the particle size roughness of gobi is ten times greater than that of dune sand, the sand threshold velocity also will increase. Sand from the Mingsha dune fills spaces between gravel particles, thus causing local sand accumulation. When the wind velocity is more than 10 ms^{-1}, the energy of the blown sand stream stimulates sand saltation. This results in erosion of the gobi.

The reason that sand accumulation and small dunes do not form is the gobi's rough surface, which decreases the capacity of sand transportation and serves as a site for the temporary arresting of sand. Because the gobi on the top

of the grottoes contains a certain percentage of sand, the sand transport rate over this surface is low. There is little energy loss due to elastic collision between sand grains and gravel particles; hence the grains in the gobi sand stream reach much greater heights, the sand flux decrease is slower, and the mean velocity of the grains is higher than that in a typical sandy desert. In addition, the sand grains can fully acquire the energy from the airflow at different heights so that the gobi sand stream is always in an unsaturated state as regards the carrying capacity of the wind. Field observations show that the sand transport rate from between 0 and 20 centimeters in height is more than 93 percent when flow velocity reaches 10.4 ms^{-1}.

Vegetation Windbreak

Figure 6 shows the vegetation windbreak on the plateau, in front of the Mingsha megadune. The airflow pattern near the shrub zone, which is 1.5 meters in average height and 50 percent permeation through the shrubs, is similar to that at the nylon wind fence, which has similar height and weave density. Based on the energy distribution, the flow pattern can be described as decelerating wind velocity that occurs before the shrub zone, decreasing speed in the shrub zone, recovering speed coming out of the shrub zone, and accelerating velocity that occurs far beyond the shrub zone. The shrub zone can obviously reduce wind speed, and a double line of shrub zones can reduce wind speed significantly. Wind speed downwind, at a distance of about twenty to thirty times the

FIGURE 6 Vegetation wind fence and drip irrigation.

Table 1   Rates of Sand Transport Upwind and Behind the Vegetation Windbreaks

Height (cm)	Upwind Sand Dune	2 m behind First Wind Break	2 m behind Second Wind break
	Sand Transport Rates ($\times 10^{-4}$ g/cm^{-2} · min^{-1})		
0~2	23.84	0.35	0.04
2~4	19.82	0.22	0.02
4~6	7.82	0.41	0.02
6~8	3.71	0.10	0.22
8~10	1.88	0.06	0.03
10~12	0.98	0.06	0.02
12~14	0.52	0.11	0.02
14~16	0.37	0.04	0.02
16~18	0.22	0.10	0.02
1~20	0.19	0.09	0.01
0~20	59.35	1.54	0.43

Comprehensive Effects of Sand Control

Through comparative determination of the quantities of sand accumulation on the walkways in front of caves 152, 208, 256, 454, 404, and 457, it was found that the sand deposits markedly decreased when the nylon fences in the gobi area were set up in October 1991 (fig. 7). During the first year, the amount of sand deposited on the walkways decreased by about 39 to 83 percent, and sand control thereafter improved yearly. Sand accumulation on the walkways increased significantly in 2000, however, for two reasons. First, sand had piled up about 1.8 meters at both sides of the fence by 1999, which reduced its sand-blocking effect. Second, sand cleaning along the northwest and southeast wind of the fence in 1997 disturbed the stable gobi surface and contributed to sand accumulation on the walkway. While still an experimental system under development, the nylon fence, vegetation barrier, and chemical stabilization of sand set up in 2003 at the cliff edge produced a decrease of sand deposition in front of the grottoes of approximately 94 to 98 percent compared to the period before the 1990s.

Conclusion

In order to significantly reduce windblown sand accumulation at the site, a multifunctional protective system (fig. 8), including engineering, biological, and chemical measures, was established over a period of some twelve years. The strategy was to reduce sand coming from the Mingsha megadune and stabilize the in situ sand on the gobi surface between the dune and the grottoes. Under the control of multidirectional winds, some sand is arrested by the gravel and some is transported by the gobi sand stream. The latter may be a threat to the Mogao Grottoes in that the sand is transported by salta-

height of the shrubs, was 40 to 70 percent of that at 30 meters upwind of the shrub zone.
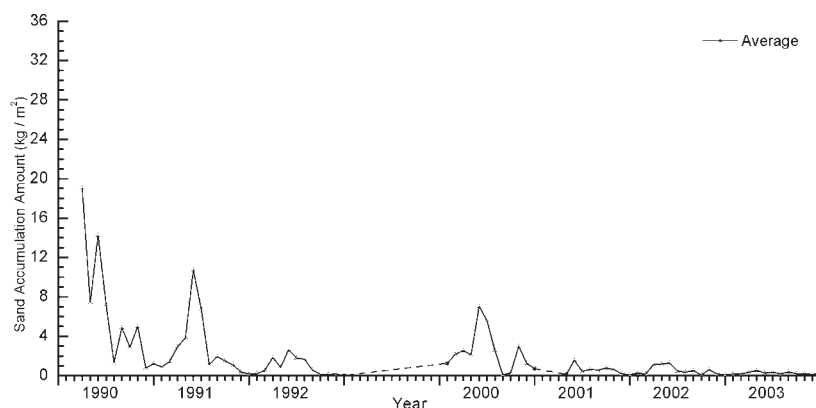
Table 1 shows the observed sand transport rates upwind and behind the vegetation wind breaks. Under a northwest wind speed of 9.8 ms^{-1}, the sand transport rates (0~20 cm high) 30 meters upwind of the shrub belt, 2 meters behind the first vegetation fence, and 2 meters behind the second are 59.35 $\times 10^{-4}$, 1.54 $\times 10^{-4}$, and 0.43 $\times 10^{-4}$ g/cm^{-2} · min^{-1}, respectively. Sand transport rates at 2 meters behind each shrub shelter belt are 1/38 and 1/138 less than the sand transport rates 30 meters upwind, showing the effectiveness of the system.

FIGURE 7 Monthly and yearly average sand accumulation in front of the caves.
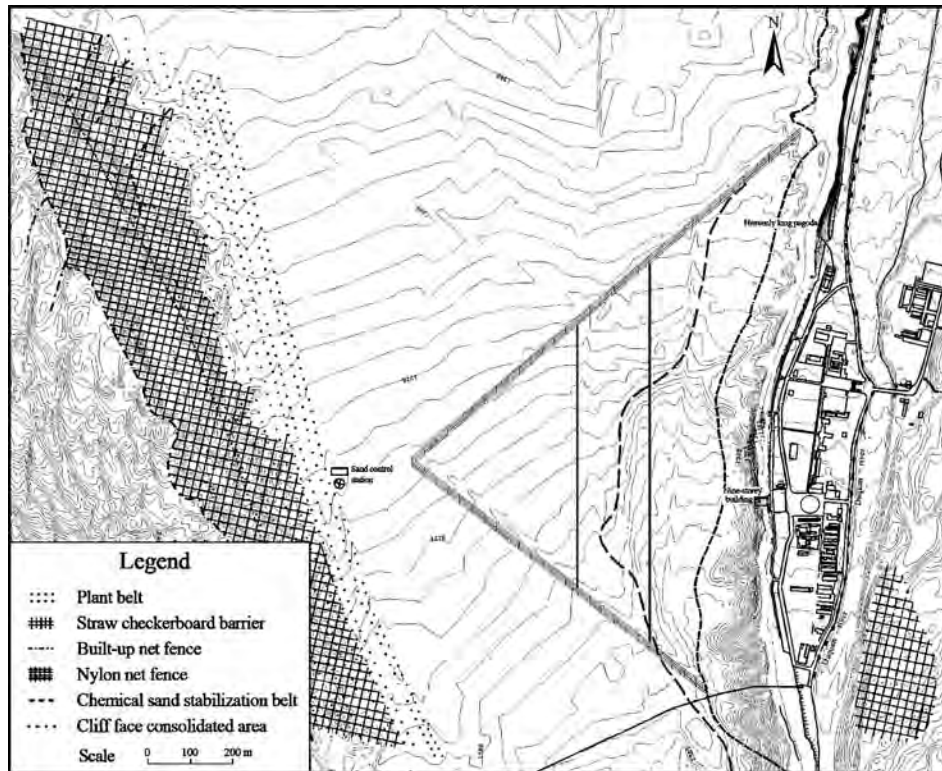
FIGURE 8 Plan of the Mogao Grottoes site showing the multifunctional sand control system.

tion. The grit gobi surface inhibits sand transport. The combination of the upright sand-block fences, half-buried straw checkerboard barriers, drip-irrigated vegetation fences, and gravel "mulch" has so far proven an effective way to protect the Mogao Grottoes from the hazards of windblown sand.

Acknowledgments

References

Dong Zhibao, Qu Jianjun, and Liu Xian. 2001. [Experimental research on the resistant coefficient on the ground surface of the Gobi Desert.] [*Science in China*] 31: 953–58 (in Chinese).

Li Zuixiong, N. Agnew, and P.-M. Lin. 1997. Chemical consolidation of conglomerate and sand at the Mogao Grottoes. In *Conservation of Ancient Sites on the Silk Road: Proceedings of an International Conference on the Conservation of Grotto Sites,* ed. N. Agnew, 194–212. Los Angeles: Getty Conservation Institute.

Lin, P.-M., N. Agnew, Li Yunhe, and Wang Wanfu. 1997. Desert-adapted plants for control of windblown sand. In *Conservation of Ancient Sites on the Silk Road: Proceedings of the International Conference on the Conservation of Grotto Sites, Mogao Grottoes at Dunhuang, October 1993,* ed. Neville Agnew, 227–34. Los Angeles: Getty Conservation Institute.

Ling Yuquan, Qu Jianjun, Fan Jinshi, and Li Yunhe. 1997. Research into the control of damage by windblown sand at the Mogao Grottoes. In *Conservation of Ancient Sites on the Silk Road: Proceedings of the International Conference on the Conservation of Grotto Sites, Mogao Grottoes at Dunhuang, October 1993,* ed. Neville Agnew, 213–26. Los Angeles: Getty Conservation Institute.

Ling Yuquan, Qu Jianjun, Fan Jinshi, Li Yunhe, N. Agnew, and P.-M. Lin. 1996. [Analysis of the effectiveness of sand control on the plateau above the Mogao Grottoes]. *Zhongguo sha mo = Journal of Desert Research* 16 (1): 13–18.

Qu Jianjun, Huang Ning, Dong Guangrong, and Zhang Weimin. 2001. [The role and significance of the Gobi Desert pavement in

controlling sand movement on the cliff top near the Dunhuang Mogao Grottoes]. *Journal of Arid Environments* 48 (3): 357–71.

Wang Wanfu, Li Zuixiong, Liu Xianwan, and Zheng Caixia. 2004. [The results of shrub belts on sand control at the top of the Mogao Grottoes]. *Zhongguo sha mo = Journal of Desert Research* 24 (3): 306–12.

Wang Wanfu, Zhang Weimin, and Li Yunhe. 2000. [A study on the impact of blown sand and its control at the Mogao Grottoes]. *Dunhuang Research* 63 (1): 42–48.

Xue Xian, Zhang Weimin, and Wang Tao. 2000. [The results of wind tunnel experiments on sand control with gravel and field monitoring: A case study at the Mogao Grottoes]. *Acta Geographica Sinica = Journal of Geographical Sciences* 55 (3): 375–83.

Zhang Weimin, Wang Tao, Xue Xian, Wang Wanfu, Guo Yingsheng, and Liu Jinxiang. 2000. [Study of a comprehensive system to control windblown sand at the Mogao Grottoes]. *Zhongguo sha mo = Journal of Desert Research* 20: 409–14.

Zhu Junfeng and Zhu Zhenda. 1999. *Zhongguo sha mo hua fang zhi.* Beijing: Zhongguo lin ye zhu ban she.

Restoration and Consolidation of Historic Earthen Structures: The Upper and Middle Temple Complexes at the Mogao Grottoes

Sun Yihua, Wang Wanfu, and Fu Qingyuan

Abstract: *The adjacent Upper and Middle Temple complexes are rare surviving examples of earthen buildings at the Mogao Grottoes. According to the inscribed plaque on the entry gate of the Middle Temple, it was built in 1772 C.E. (during the Qing dynasty, in the thirty-seventh year of Emperor Qianlong's reign). At Dunhuang, an arid region, most of the buildings were made of earth. After some two hundred years, the walls of the temples had deteriorated; this has been especially rapid over the past twenty years as the buildings were left unoccupied and not maintained.*

The principle followed for conserving and restoring the temple buildings specifies that after restoration the structures should retain as much of the original fabric as possible. The conservation plan comprised three parts: (1) collapsed and nonextant structures were to be reconstructed based on their foundations and knowledge of the surrounding buildings; (2) for partially collapsed buildings, the collapsed areas were to be reconstructed and the rest of the buildings restored and stabilized; and (3) for the relatively intact buildings, only the lower parts of walls were to be restored and strengthened.

During restoration, an invisible, impermeable layer was added to the footings of the buildings. Based on information gained from historical traces and remains, windows and doors were restored to their 1944 condition. The restoration was completed in June 2003, and today the temples display their historic appearance. Through this project, a way of conserving deteriorated earthen buildings was developed. Both the approach and the techniques are new and in compliance with the China Principles.

As an important World Heritage Site on the Silk Road, the Mogao Grottoes, with their exquisite mural art and statuary, have received considerable attention. In addition to the grottoes, many buildings, primarily monasteries and temples, were originally constructed over a period of more than a thousand years, beginning in about the fourth century C.E. According to the historical record, there were many ancient monasteries and temples at Mogao Grottoes. Today, only a few temples from the Qing dynasty survive at the site. These include the Upper and Middle Temples (so called because of their location in relation to the grottoes along the cliff face) and two earthen buildings only 50 meters from the grottoes. Each temple is a complex of buildings. Together, the temples contain twenty-five buildings with a total of eighty-one bays (a Chinese ancient building unit). After being exposed to the elements for more than two hundred years, the earthen walls of the Upper and Middle Temples have weathered and deteriorated. This situation has worsened over the past twenty years when the buildings were unoccupied and not maintained (fig. 1).

The deteriorated temples were eyesores, and their significance and conservation needs attracted the interest of colleagues from the Getty Conservation Institute and the Australia Heritage Commission. Experts from both institutions visited the temples in 2000 and proposed a treatment plan based on the China Principles (Agnew and Demas 2004) to stabilize the buildings and restore them to their original appearance (fig. 2).

The structures themselves are not architecturally significant, so why should we conserve them now? Because they housed the first state-sponsored conservation and research institute, the National Dunhuang Art Research Institute. Established in 1944, this institute later became the Dunhuang Academy. The buildings were used as offices,

FIGURE 1 Deteriorated north wall of a building in the Upper Temple before restoration.

FIGURE 2 The north wall shown in figure 1 after restoration.

work areas, and staff quarters until the late 1970s. Thus the temples are historic structures owned by the state, and they signify the transformation of commonplace constructions to commemorative ones.

Values Assessment and Investigation

The Upper and Middle Temples are two small building complexes next to each other, typical of the local mud-brick, flat-roofed style. There are several very old elms inside the courtyards. The gate of the Upper Temple is inscribed with the words *Lei Yin Temple,* but this inscription and a couplet on both sides of the doorframe are scarcely visible.

A wooden plaque from the gate of the Middle Temple, bearing the words *Lei Yin Chan Lin* (the name of the temple complex), is dated to the thirty-seventh year of Emperor Qianlong (1772). The words on the back of the plaque explain that the temple was rebuilt with collected alms; therefore, it must have been built before the year 1772. The plaque is now housed in the Dunhuang Academy's cultural artifacts storage area.

The two temple complexes are similar in scale and layout. The building walls were made of mud brick, without sill wall bricks. All north-facing rooms and side rooms were constructed with flat roofs, while small post-and-beam structures were used for the main rooms.

When the newly formed National Dunhuang Art Research Institute moved into the temples in 1944, the rooms were altered to accommodate staff (some fourteen families in all) and to serve as offices. When the institute moved to a new building and became the Dunhuang Academy, the abandoned temples were seriously damaged by weathering, and parts of the temples collapsed. Branches of the old elms also endangered the roofs. Leaking water rotted the wooden supports under the roofs. Piles of rubbish that had accumulated at the foot of the buildings over the years led to rotting of the column bases. The mud plaster fell from the walls, exposing the mud bricks and subjecting the walls to salt efflorescence and cracking.

Prior to conservation, only seven buildings were in good condition—those that served as the residence of Chang Shuhong, first director of the National Dunhuang Art Research Institute. In other parts of the temples, 15 bays had completely collapsed, the walls and beams of 39 bays had partially collapsed, and 20 bays were on the verge of collapse. In fact, some walls did collapse soon after the conservation project began, between winter 2001 and spring 2002.

Treatment Plan

Before conservation work began, the site was excavated to investigate the foundation of the collapsed buildings and establish the original levels of the courtyard and rooms. Archaeological data were supplemented with information about the original condition of the temple buildings obtained from interviews with people who had worked or lived at the site, from old photographs, and from old survey drawings.

The treatment plan was as follows:

1. Collapsed temple buildings would be rebuilt as close to their original condition as possible, based on the archaeological data; information obtained

from interviews, photographs, and survey documents; and using appropriate materials and traditional building techniques. The intent was to integrate the reconstructed components with the remaining ones.

2. For partially collapsed buildings, the collapsed areas would be reconstructed and the rest of the buildings restored and stabilized.

3. For the relatively intact buildings, only the lower parts of walls would be stabilized and strengthened.

The guiding principle for the conservation and restoration of the temples was that the structures should retain as much of the original fabric as possible. This approach is consonant with the China Principles guidelines and the heritage laws of China. A document from the State Administration of Cultural Heritage (SACH; formerly the State Bureau of Cultural Relics) specified how the work should be done: "For walls with efflorescence and cracks, the key point is to repair and reinforce the damaged parts; no excessive changes are allowed. Conservation of the floor tiles, decorations, nails and the nail holes on the walls, the pictures and bulletin boards should also receive attention. . . . And it is advisable to select local traditional materials for decorating houses and walls" (SACH 2001).

These treatment plan goals added to the difficulty of the project in that the work involved a conservation approach rather than one that adopted reconstruction as the guiding principle. Continuous testing was therefore necessary before appropriate treatments were decided on.

Restoration of the Upper Temple Complex

Restoration of building No. 10 in the Upper Temple complex is presented here to show the project's challenges and activities.

Prior Alterations and Damage

Zhang Daqian, a famous painter, had lived in building No. 10 at the northeast side of the Upper Temple from 1942 to 1943 and, according to the recollection of several people interviewed, had created a painting on one of the walls in a room. Other people later occupied the room, and the painting was covered with whitewash many times. After the temple complex was abandoned, it quickly deteriorated. Many serious problems were apparent before the project began. Apart from the types of general deterioration already mentioned, a fire

had damaged the west wall of this building; modifications, such as conversion of a window into a fireplace, had been undertaken; new windows had been installed; and so on.

Repair

The general types of interventions undertaken during the project are described below.

Replacement of a Wall Foundation. Wooden boards and frames were used to support damaged walls before the deteriorated lower parts were undercut. The extent of cutting was based on the degree of deterioration. Wooden boards were used at the upper part of the cutting to support and stabilize the upper walls. During this procedure a trench about 1.5 meters long, 1.5 meters deep, and 1 meter wide was dug along the wall base. After the old footing was removed, the base of the trench was compacted. Then concrete was poured to form a foundation, after which a new footing of red brick was built. When the new footing reached ground level, a wall base was made of lime mortar and gray bricks (on the inner side of the wall there was one course and on the outer side three courses). Above the new base, mud plaster mixed with straw and adobe bricks that had been soaked in potassium silicate solution for added strength and durability were used to build up the base until it almost reached the bottom of the original wall, leaving a gap of about 1 centimeter. Then a 1:1 ratio of cement and clay mixture was used to fill the gap tightly. After the replacement was complete, the wall was plastered with a mixture of mud and straw, according to the original materials and technique used (fig. 3).

FIGURE 3 Wall stabilization with a brick footing.

Restoration of a Tilted Structure. The wooden framing and the gable springer for the earthen walls were returned to their original state at the same time. Securely propping up the walls involved great danger and difficulty. Walls that were not vertical or had subsided were corrected using a jack. Prior to being jacked up, the wall was supported, framed, and undercut following the procedures used for replacing the foundation of a wall. After the wall was pushed back to the vertical position, its footing and foundation were built up according to the procedures described above.

Repair of the Roof, Wall, and Surface. Since the roof was essentially intact, only a few changes were made during repair. The original layer of clay and straw covering the roof was removed, and a 2-centimeter-thick layer of new roof boarding and a felted waterproof layer were added over the original roof boarding. Then a layer of mixed clay and straw was added over the waterproof layer. This was reinforced by spraying with potassium silicate solution.

As mentioned, it was said that Zhang Daqian had executed a painting on the wall, but the exact place was not known. Removal of the coatings layer by layer revealed an ink painting of bamboo on the back wall, about 2 to 3 square meters in size. The surface was full of small pits that had been made so that the wall could be plastered. All the walls inside were likewise uncovered to expose this layer, and the pits were filled.

Grout containing potassium silicate was used to strengthen the bond between the original adobe bricks and between the adobe bricks and the plaster layer, during which cracks and detachments were also repaired. The procedure for grouting cracks was as follows: (1) the crack was sealed on both sides of the wall, leaving a hole at an appropriate location to insert a grouting tube; (2) grout was then injected starting at the lower part of the crack and moving upward; and (3) after the tube was removed, the grout hole was sealed. The procedures for grouting cracks and detachments were identical, except that a presser was added to support the grouted area when detachments were repaired.

Decorative Carpentry. Although some structures had been restored many times, vestiges of the original wooden windows remained, and these were repaired with wood. When all the structures were finished, some work was done to make them look old and in harmony with the roof and wall.

Restoration of the Middle Temple Complex

The doors and windows of the two temples were repaired differently, reflecting their different uses over time. After 1943, when the Middle Temple became the office of the National Dunhuang Art Research Institute, the windows and doors were greatly changed. There were no radical or extensive changes to the Upper Temple. Therefore, the windows and doors of the Upper Temple were restored to their original form, and those of the Middle Temple remained in their modified forms from the 1950s and 1960s.

Restoring building No. 20, a wing house in the north of the backyard of the Middle Temple, was a key task since it had been the residence of Chang Shuhong, first director of the institute. This restoration was left to a later stage of the project. Other than repairing the earthen *kang* (heated bed), bookcase, and bookshelf (both also earthen), little else was done so that the hardships experienced during those early

FIGURE 4 Chang Shuhong's residence before restoration.

FIGURE 5 Chang Shuhong's residence in the 1940s, after the removal of nonoriginal interventions.

times could be preserved as witness to the early history of the Dunhuang Academy. Thus we achieved the aim of "restoring the relics to their original appearance" (figs. 4, 5).

Additional Restorations

Among the additional buildings restored during the project were a row of stables to the north of the Middle Temple and a mill room between the two temples. The stables were converted into a dormitory for employees after 1944 and have been in use ever since. The mill was a factory where the food for all the workers of the institute was processed.

Summary

In June 2004, after nearly two years of work and with support from leaders at all levels, the conservation of the Upper and Middle Temple complexes at the Mogao Grottoes was completed. This project was a new approach to repairing commemorative structures made of mud brick. The three groups taking part in the project—the Dunhuang Academy, the Getty Conservation Institute, and the Australia Heritage Commission—had no prior experience with this type of con-servation, but through cooperation and hard work, the project was skillfully finished and recognized as such by those who had supported it.

On November 1, 2003, experts from the Gansu Provincial Cultural Bureau inspected and accepted the work done at the two temples. They commended the work, stating, "In the project, the original materials, structures, and techniques were strictly retained, and the cultural relics preserved to the largest extent. Repair of the surviving earth walls provides a new way and new techniques for conserving earthen constructions."

References

Agnew, N., and M. Demas, eds. 2004. *Principles for the Conservation of Heritage Sites in China = Zhongguo wen wu gu ji bao hu zhun ze [Chinese-language document] issued by China ICOMOS; approved by the State Administration of Cultural Heritage.* Los Angeles: Getty Conservation Institute.

State Administration of Cultural Heritage (SACH), PRC. 2001. Document No. 890, addressed to the Dunhuang Academy.

Consolidation Studies on Sandstone in the Zhongshan Grotto

He Ling, Jiang Baolian, Zhou Weiqiang, and Zhen Gang

Abstract: *The Zhongshan Grotto is located in Yan'an district, Shaanxi province. The grotto was created initially in the Eastern Jin dynasty, dating from 366 C.E., and was worked again during the Song dynasty (1067). The grotto was excavated out of a fine-grained sandstone rich in the mineral feldspar. The grotto and its statues show different degrees of weathering, primarily at ground level and up to 2 meters in height. The grotto rock shows severe friability and exfoliation, the color on the rock surface has faded, and cracks and fissures have occurred. As a result, many statues have only blurred outlines.*

This paper describes the factors and mechanisms contributing to weathering of the grotto. X-ray diffraction, thin section analyses, and scanning electron microscopy identified the physical and mechanical properties of the sandstone. In addition, a fluorinated polymer and two silicon compounds were used in a consolidation study. The effectiveness of the fluorinated polymer for consolidating the sandstone was systematically examined for polymer formation, penetration depth, porosity, capillary and osmotic coefficient, water uptake, compressive strength, absorption of water vapor, water vapor permeability, color changes, thermal expansion cycles, freeze-thaw cycle testing, and accelerated weathering in 10 percent sulfuric acid. The results show that the fluorinated polymer satisfied chemical and freeze-thaw resistance, and the rock remained stable in dimension. When the consolidant penetrated the sandstone to more than 5 centimeters in depth, the strength increased significantly and was evenly distributed with depth. We conclude that an appropriate concentration of the fluorinated polymer provides ideal consolidation of the Zhongshan sandstone.

The Zhongshan Grotto is located 60 kilometers from Yan'an, in northern Shaanxi province. It is an important historic grotto on the Silk Road that was first carved in about 366 C.E. during the Eastern Jin dynasty and worked again in 1067 C.E. during the Song dynasty. Since 1988 the Zhongshan Grotto has been listed among the key cultural sites of China. There are five caves and three gates carved into the mountain, and they face south toward the Xiu Yan River, following tradition. Eight carved stone pillars support the stone roof of the main cave, which contains an 11.5-meter-wide Buddha altar situated 5 meters from the entrance (fig. 1). There are sixteen Buddha figures carved out of the wall surrounding the altar, and these figures are well painted.

FIGURE 1 Buddha altar and carved stone pillars in the main cave of the Zhongshan Grotto.

The grotto is excavated out of a porous fine-grained sandstone rich in the mineral feldspar. The sandstone is gray, with some dark brown marks. Because of the grotto's location in the severe environment of northern China and its exposure to wind erosion, the stone surface has deteriorated seriously. Humidity combined with salts is another deterioration factor. Water migration has caused salts to accumulate in the rock, producing crystals that weaken the bonding between the sandstone grains. This deterioration results in heavy efflorescence on the rock surface, loss of the surface layers, loss of the binding materials between the grains of quartz, powdering of the stone, loss of detail of the sculpture, fading of the wall painting, and many fissures or cracks in the cave wall. The greatest deterioration is seen 2 meters above the ground, resulting from the capillary rise of water in the sandstone and the windy environment. This is especially noticeable on the side of the cave that backs to the mountain.

The aim of our work was to investigate the deterioration of the sandstone in Zhongshan Grotto and to study the effect of several consolidant materials on the physical, mechanical, and thermal properties of the sandstone to see how they compensate for the loss of the natural binding materials from the stone. The physical, mechanical, hygric, and thermal properties were determined for treated and untreated samples of the sandstone materials. The following were examined: polymer formation time, penetration depth, porosity, capillary absorption and penetration coefficient, water uptake, compressive strength, drilling resistance, water vapor diffusion, color changes, and resistance to disaggregation by water and freeze-thaw cycles. In addition, the effect of acid deterioration (i.e., accelerated weathering) was assessed. An in situ demonstration of several consolidants was conducted in a second cave at Zhongshan Grotto.

Samples

Samples were taken both from the sandstone surface inside the main cave and from the unweathered sandstone. Samples of salt efflorescence were obtained by scraping the weathered and unweathered surface with a small knife. Thin-section samples were taken in the same place. About 150 small stone block samples were also taken from outside the grotto. The samples measured 5 by 5 by 0.5–1.5 centimeters, 5 by 5 by 8–15 centimeters, and 5 by 5 by 5 centimeters. Each measurement was repeated at least three times, and the average value is quoted in each case.

Deterioration Study

Analytical Methods

X-Ray Diffraction (XRD) Analysis. For XRD analysis, samples were ground into a fine powder in an agate mortar and pressed into the specimen holder, then mounted in a D/MaX-rA X-ray diffractometer. Operating conditions were Cu target; 45 kV; 80 mA current; speed, 0.1; chart, 5; time constant, 1; monochromatic system, graphite.

Thin-Section Analysis. Sandstone samples were sectioned and polished, then mounted on microscope slides. The grain structure, texture, grain size, grain shape, grain contact, matrix, pores, composition, and so on were identified using a polarizing microscope.

Salt Analysis. The scraped samples of salt efflorescence were ground into a fine powder in an agate mortar after sand grains were removed (under the microscope) and then were analyzed by XRD. Diffraction patterns were interpreted by comparison with Joint Committee for Power Diffraction Standards (JCPDS) data.

Accelerated Weathering Analysis. The aging of samples was performed after a four-week interval of treatment. Fifty freeze-thaw cycles were used. Each cycle consisted of soaking the sample in water for 4 hours at 20°C to 25°C, removing it from the water and freezing it for 4 hours at −4°C to −10°C, and then soaking it in water again for 4 hours at 20°C to 25°C. A total of fifty thermal cycles were used. Each of these cycles consisted of heating the sample for 4 hours at 100°C to 110°C, cooling for 4 hours at 20°C to 25°C, and then drying again for 4 hours at 100°C to 110°C. Erosion in sulfuric acid was carried out by immersing the samples in 10 percent acid for one week.

Deterioration Study Results and Discussion

Thin-Section Analysis

The composition and properties of the weathered and unweathered samples determined by thin-section analysis are presented in table 1. The results show that both sets of samples belong to a feldspathic sandstone family. The main composition is quartz, 30 to 45 percent; plagioclase feldspars, 25 to 30 percent; hematite, 1 to 2 percent; chlorite, <1 percent; and mica, 3 to 5 percent. The sand grains were rhombus or subrhombus in shape. Because the grain size is small, about 0.25 to 0.09 millimeter, the Zhongshan sandstone is defined as fine grained. Clay fills the pores of the sandstone, but the

Table 1   Description of Thin Sections

Sample	Description of Thin Sections
Unweathered stone	Class: fine feldspathic sandstone with grain size 0.25–0.09 mm
	Composition: quartz 30–45%, plagioclase feldspar 25–30%, chlorite <1%, hematite 1–2%, mica 3–5%
	Filler: mica clay and ferric minerals
	Porosity: 10–15% with pore size from 0.1 mm to several mm
Weathered stone	In general, similar to unweathered stone with the following exceptions: (1) less ferric minerals and (2) more pores with smaller pore size

Table 2   XRD Analysis Results for Zhongshan Sandstone

Sample	Mineral Composition
Unweathered	Quartz: 44%; sodium feldspar: 32%; illite and smectite: 5%; siderite: 5%; chlorite: 4%; kaolinite: 3%; microcline: 3%; zeolite: 2%; other: 2%
Weathered	Albite feldspar: 38%; quartz: 32%; microcline feldspar: 8%; chlorite: 7%; illite: 5%; calcite: 5%; zeolite: 2%; other: 3%

ferric minerals are within the grains. In thin section, the weathered sample contains less ferric mineral and has more pores with smaller pore size than the unweathered samples.

XRD Analysis

The results of XRD analysis of unweathered sandstone samples are similar to those obtained from thin-section analysis: quartz, 44 percent; sodium feldspar and microcline, 32 percent + 3 percent; with trace amounts of other minerals, totaling 21 percent. For the weathered samples, the amount of feldspar increases to about 46 percent (albite feldspar and microcline feldspar), quartz is at 32 percent, and chlorite is a bit high at 7 percent. See table 2.

Causes of Deterioration

Clays. The structure and composition of the sandstone show that it deteriorates easily in the local environment. Clay minerals from weathered feldspar swell with water, especially smectite $(Al_2[Si_4O_{10}](H_2O)_2 \cdot nH_2O)$. Smectite contracts on drying. Repeated swelling and contraction destroys the strength of the sandstone and produces cracks. All of these actions contribute to the powdery and sandy nature of the weathered sandstone in the Zhongshan Grotto.

Porosity and Pore Size. In addition, the porosity and pore size of the sandstone make it possible for water to penetrate the rock, dissolving some minerals. This also reduces the rock strength. The larger porosity and smaller pore size of the exterior stone are a typical consequence of dissolution by water.

Salts. Soluble salts in sandstone also play an important role in the deterioration process. XRD analysis results revealed that salts can be dissolved, transported to, and then leached from the surface of the stone. Salt crystallization-dissolution cycles occur with humidity changes in the dry, cold environment of the Zhongshan Grotto. This process also results in cracks, fissures, powdering, and flaking of the sandstone.

Water movement and salt precipitate were inferred from the presence of decomposition of kaolinite and the increase of albite in XRD analysis. This confirmed the role of chemical weathering in the deterioration of the stone, with the resulting transformation of the constituent minerals into other minerals more susceptible to mechanical strain and dissolution. Even quartz, one of the most durable minerals, showed susceptibility to mechanical deformation as a result of stress from static or dynamic loads.

On the other hand, the crystallization-dissolution cycles of salts, together with the typical windy weather in the region, have altered the pigments inside the Zhongshan Grotto such that many areas of the painted figures in the main cave have become black (fig. 2), or only a vague outline of the image remains because of soluble salts (fig. 3). The paint was applied directly to the stone surface. Paint layers have peeled off, and binding materials have likely deteriorated.

Salts are a powerful weathering agent, especially when combined with freezing temperatures. The Zhongshan Grotto is located in a region where the temperature in winter is often −20°C, so freezing is a serious contributor to deterioration.

All these factors, either endogenous from the physical and chemical properties of the stone or exogenous from the surrounding environment, are able to transform the sandstone from a hard, strong, coherent state into a completely

FIGURE 2 Painted figures blackened by deterioration.
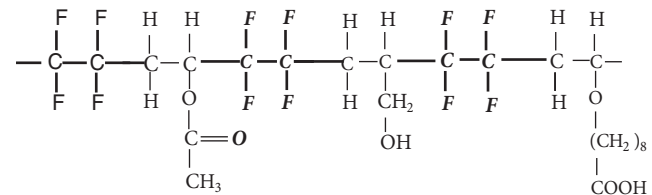

FIGURE 3 Figure eroded by soluble salt and water.

disintegrated, weak state. This will lead ultimately to complete destruction of the stone in the future.

In the second part of our investigation, described below, we tested several consolidants as a substitute for the natural binding materials. It is to be expected that the friable sandstone treated with these consolidants will gain new properties, becoming more resistant to deterioration in the future. Several of the most promising consolidants were then evaluated during an in situ demonstration in a second cave.

Consolidation Study

Experimental Consolidants

The consolidants used were a fluorinated polymer and organosilicon materials. Fluorinated polymers are well known for their excellent weathering and oxidation resistance and the mechanical properties they impart to stone (Mclain, Sauer, and Firment 1996; Alessandrini, Toniolo, and Colombo 2000; Ciardelli et al. 2000). These characteristics directed our attention to this kind of polymer for the consolidation study. We synthesized a multifunctional and partially fluorinated polymer, called F4-SS (F = fluorinated-containing, 4 = four monomers, SS = stone strengthener), specifically for sandstone conservation (He Ling and Liang Guozheng 2003). This is a copolymer prepared with four monomers: tetrafluoroethylene (C_2F_4), vinyl acetate ($CH_3COOCH:CH_2$), allyl alcohol ($CH_2:CHCH_2OH$), and 10-hendecenoic acid ($CH_2:CH(CH_2)_8COOH$). The F4-SS copolymer formula is shown below.

F4-SS has a strong ability to combine with the minerals in sandstone, achieves sufficient penetration depth, and provides essential consolidation strength. The important point is that it is soluble in common solvents, and it has a high glass transition temperature (He Ling and Liang Guozheng 2003). F4-SS was used at concentrations of 5 percent, 20 percent, and 30 percent in butyl acetate (ASTM C67-97 1997).

Two organosilicon compounds (Remmers 300 and WD-02) and mixtures of F4-SS + WD-102 were also used as consolidants to compare their properties.[1]

Experimental Method

Sandstone samples were cut into cubes (5 cm³) and dried in an oven at 105°C for 24 hours until constant weight, then cooled to room temperature and 55 percent relative humidity for half an hour and weighed again.

Two consolidation methods were used in this study: capillary absorption parallel to the bedding plane and capillary absorption perpendicular to the bedding plane. After the consolidant was applied, it was allowed to cure for four weeks before analysis.

Treatment Evaluation

Gel Formation and Penetration Depth. Gel formation of the different consolidants was determined by weight change of the treated samples after four weeks of curing. The penetration depth of the applied consolidants was measured by capillary rise through the 5-cubic-centimeter cubes.

Hygric Properties. Porosity, water uptake, hygric dilatation, water absorption coefficient, water penetration coefficient, water vapor diffusion, and water vapor absorption were determined according to ASTM C67-97 (1997) for the treated and untreated samples.

Color Change. Evaluation of color changes between the treated and untreated samples was carried out with a MINOLTA CR-300 colorimeter.

Compressive Strength and Accelerated Weathering. After four weeks of curing, treated and untreated samples were subjected to fifty freeze-thaw cycles, thirty heat cycles at 100 to 110°C, and 10 percent H_2SO_4, and then compressive strength was determined. Compressive strength was determined according to ASTM C67-97, with the load applied perpendicular to the bedding plane. Compressive strength before and after aging was measured for treated and untreated samples.

Scanning Electron Microscope (SEM) Analysis. To evaluate the effects of the consolidants, the treated and untreated samples were examined by SEM analysis using a HITACHI S-570. The samples were coated with gold to a thickness of 110 nanometers. The SEM micrographs were also examined to find the difference before and after aging.

Consolidation Study Results

Gel Formation and Penetration Depth

Figure 4 shows the gel formation over the four-week curing process. Samples treated with F4-SS had a constant weight after two weeks, but the samples treated with Remmers 300 and WD-02 needed at least a month to achieve constant weight. The initial absorption of the F4-SS was proportional to the viscosity of the preparation used. Because the 5 percent solution has the lowest viscosity, it had the largest absorption; conversely, the 30 percent high-viscosity solution had the least absorption. But the final gel content is proportional to the concentration of fluorinated polymers. The amounts of Remmers 300 and WD-02 absorbed by the samples were more than the amount of F4-SS absorbed because of their higher concentration.

Table 3   Consolidant Penetration Depth Measured by Capillary Rise through Sample

Consolidant	Penetration Depth (cm)		% Increase
	At 10 Min.	At 4 Weeks	
5% F4-SS	2.5	4.1	64
20% F4-SS	1.5	5.0	233
30% F4-SS	3.4	3.6	6
WD-02	2.2	3.2	45
Remmers 300	2.3	3.1	35

The penetration depths of the consolidants were compared by measuring capillary rise through the 5-cubic-centimeter cubes. Table 3 presents the results. It was found that the depth after four weeks was two to three times greater for the F4-SS solutions, although the capillary absorption of samples of 5 by 5 by 8–15 centimeters was carried out within the same time. The 20 percent F4-SS increased the most after four weeks; the 30 percent F4-SS, the least due to its higher viscosity and due to its polymerization at the surface of the stone sample. The mixed polymer of F4-SS + WD-10 performed similarly to the 20 percent F4-SS. WD-02 and Remmers 300 gave about 45 to 35 percent increase in penetration depths.
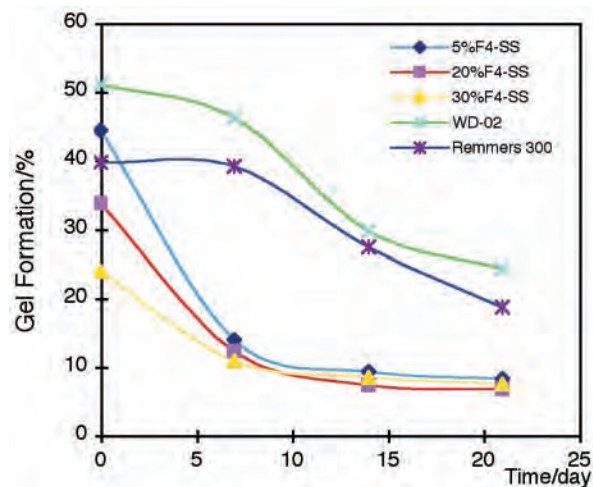

FIGURE 4 Gel formation over the four-week curing process.

Hygric Properties

Porosity and Water Uptake. Porosity of the treated and untreated samples was determined according to ASTM C97 (table 4). The results indicated that the porosity of all samples, either under vacuum for 24 hours or in boiling water for 5 hours, was nearly the same. The higher the concentration of F4-SS, the more the porosity decreased for treated samples. At 5 percent F4-SS, there was little reduction in porosity compared with that of untreated stone because a very thin film formed on the mineral surface and after the solvent evaporated. The film thickness in the pores increased with the concentration of F4-SS, and the porosity decreased. In addition, porosity is related to the test method: fluorinated polymer has a significant hydrophobic property, which can cause the porosity to be relatively lower.

Water uptake is the water absorption under atmospheric pressure for 24 hours. Water absorption of the treated and untreated samples was determined according to ASTM C97 (see table 4). The variation in water uptake showed exactly the same tendency as porosity because porosity is closely related to water uptake and water transport. The water uptake of the mixed system F4-SS + WD-10 was lower because of the addition of WD-10, a long-chain organosilicon that has a significant hydrophobic effect.

Water Absorption and Penetration. The influence of capillary processes in stone is expressed by the water absorption coefficient (W) and the water penetration coefficient (B). Values obtained for W and B in our consolidation study are given in table 4. All treated samples showed a decrease in W and B values compared with the untreated sample. The W and B values decreased with increasing fluorinated polymer content: 30 percent F4-SS showed extremely low W and B values. WD-02 and Remmers 300 performed similarly. The mixed system of F4-SS + WD-10 showed a decrease in capillary absorption, penetration, and porosity, and the degree of decrease was proportional to the concentration of WD-10.

Hygric Dilatation. Cracking and flaking of stone are caused by swelling due to water absorption. Dilatation was measured for all the samples. The results are given in table 4. It is clear that dilatation correlates with W and B values. Samples treated with 20 to 30 percent fluorinated polymers showed less dilatation than those treated with the silicon polymers (WD-02 and Remmers 300). The mixed system of F4-SS + WD-10 gave a value between those of the two separate polymers.

Water Vapor Diffusion. Water vapor diffusion, μ, measures water vapor movement through a medium. The higher the value of μ, the more difficult it is for water vapor to diffuse through the medium. At all three concentrations, F4-SS had similar diffusion values. Adding WD-10 to the F4-SS slows diffusion. Experiments showed that the sample surface remained dry when pure F4-SS was used; however,

Table 4   Hygric Properties of Stone Samples

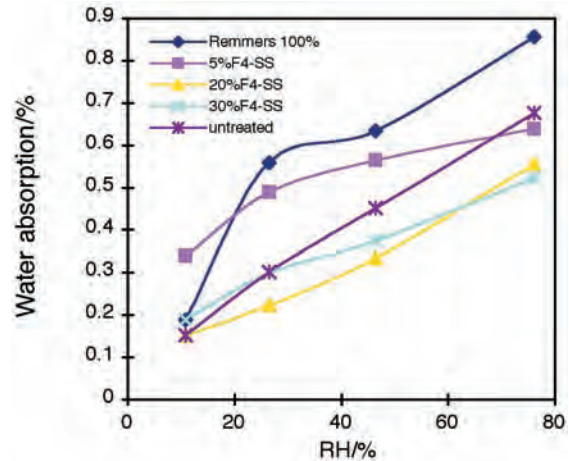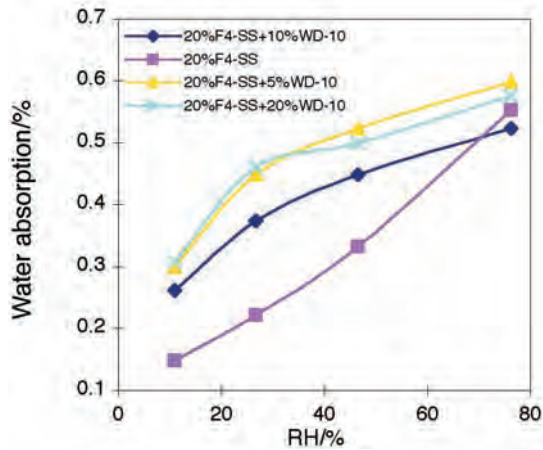| Consolidant	Porosity (%)	Water Uptake (%)	Water Absorption Coefficient, W ($kg \cdot m^{-2} \cdot h^{-1/2}$)	Water Penetration Coefficient, B ($cm \cdot h^{-1/2}$)	Hygric Dilatation (μmm^{-1})	Water Vapor Diffusion (μ)
5% F4-SS	9.3	8.40	2.02	1.02	1193	7.37
20% F4-SS	7.7	8.01	0.28	0.79	395	9.07
30% F4-SS	4.4	5.72	0.03	0.01	791	10.15
20% F4-SS + 20% WD-10	0.9	3.38	0.06	0.21	791	16.93
20% F4-SS + 10% WD-10	4.2	3.03	0.16	0.01	790	9.80
20% F4-SS + 5% WD-10	2.5	3.36	0.08	0.16	1197	27.62
WD-02	6.2	6.94	1.07	3.28	1188	11.59
Remmers 300	5.8	8.20	1.18	1.4	1179	7.61
Untreated	16.8	9.17	4.10	3.29	1296	7.03

FIGURE 5 Water vapor absorption isotherms for different consolidants.

water drops accumulated on the surface when a mixture of F4-SS and WD-10 was used. This indicated that water vapor was unable to diffuse through the sample, and water drops were formed on the rock surface. Table 4 shows the results of these tests.

Water Vapor Absorption Isotherm. Different relative humidity environments were generated using four saturated salt solutions: 11 percent (LiCl), 35 percent (MgCl$_2$), 58–60 percent (NaBr), and 76 percent (KHSO$_4$). Figure 5 shows the water vapor absorption isotherms. Remmers 300 exhibited the largest water vapor absorption above 20 percent RH. The three fluorinated polymer concentrations did not significantly affect the samples, and treated samples exhibited water absorption similar to that of the untreated sample. The addition of WD-10 results in a little more water absorption than that achieved with the pure fluorinated polymers.

Color Variation. Figure 6 shows the color variation of samples treated with several consolidants. The results were obtained by comparison with an untreated sample. WD-02 caused the most color change; the fluorinated polymers and Remmers 300 caused a small amount of color change.

Compressive Strength and Accelerated Weathering. Compressive strength measurements were carried out at different stages for treated and untreated samples: at four weeks after treatment, after fifty freeze-thaw cycles, after thirty heat expansion cycles at 100°C to 110°C, and in 10 percent H$_2$SO$_4$. Average values of compressive strength are listed in table 5.

The untreated samples had an average compressive strength value of 47 MPa. After the treated samples were allowed to cure for four weeks, those treated with 30 percent F4-SS had the highest value: 89 MPa. WD-02 and

Remmers 300 had high values because of their 100 percent concentration, without dilution with solvent.

After fifty freeze-thaw cycles, samples treated with all three concentrations of F4-SS showed the smallest percentage decrease in compressive strength, about −16 to −37 percent, as shown in table 5, while those treated with mixtures of F4-SS + WD-10 showed the largest decrease percentage, −50 to −75 percent. Results for samples treated with WD-02 and Remmers 300 lay between these two ranges. During the freeze-thaw cycles, the sample treated with 20 percent F4-SS + 20 percent WD-10 cracked in forty-two cycles, and the sample treated with 20 percent F4-SS + 10 percent WD-10 cracked in thirty-five cycles.

After thirty thermal expansion cycles, the sample treated with 5 percent F4-SS was the only one that showed an
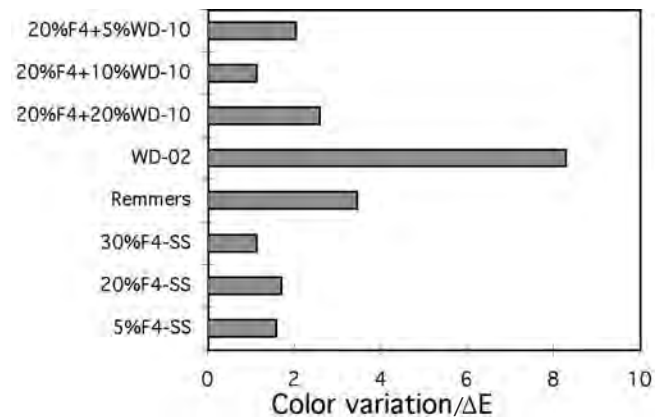

FIGURE 6 Color change measured for different consolidants.

Table 5   Compressive Strength Test Results

Consolidant	Compressive Strength (MPa)*			
	At 4 Weeks Posttreatment	After 50 Freeze-Thaw Cycles	After 30 Thermal Expansion Cycles	After Erosion in 10% H$_2$SO$_4$
5% F4-SS	52.64	44.30 (−15.8)	55.35 (+5.2)	41.24 (−21.7)
20% F4-SS	61.83	49.47 (−20)	49.21 (−20.4)	56.77 (−8.2)
30% F4-SS	88.86	56.29 (−36.6)	63.73 (−28.3)	61.27 (−31.0)
20% F4-SS + 20% WD-10	73.28	23.51 (−67.9)	44.84 (−38.8)	36.99 (−49.5)
20% F4-SS + 10% WD-10	43.65	10.93 (−74.9)	30.56 (−30)	32.18 (−26.3)
20% F4-SS + 5% WD-10	71.20	31.62 (−55.6)	58.33 (−18.1)	32.16 (−54.8)
WD-02	81.53	49.70 (−39.1)	71.43 (−12.4)	40.41 (−50.4)
Remmers 300	83.47	45.04 (−46)	71.82 (−13.9)	41.57 (−50.2)
Untreated	47.29	42.38 (−10.4)	43.25 (−8.5)	32.31 (−31.7)

*Numbers in parentheses indicate % increase (+) or decrease (−) in compressive strength.

increase in compressive strength (+5%); all other treated and untreated samples had decreased values.

These results indicate that samples treated with WD-02 and Remmers 300 have better thermal resistance than those treated with fluorinated polymers, but they have poorer H$_2$SO$_4$ erosion resistance. These results can be explained by the property of consolidant mixtures. A 5 percent F4-SS mixture contains much more solvent than the others. Continued polymerization occurred during drying at 100°C to 110°C, causing an increase in compressive strength. When samples were treated with 30 percent F4-SS, polymerization occurred at the sample surface, but the temperature of drying samples in 100°C to 110°C is higher than the glass transition temperature (T$_g$) of F4-SS polymer, so the film softened and caused the decrease in compressive strength. Samples treated with WD-02 and Remmers 300 showed good thermal resistance because of the chemical combination between polymer and stone.
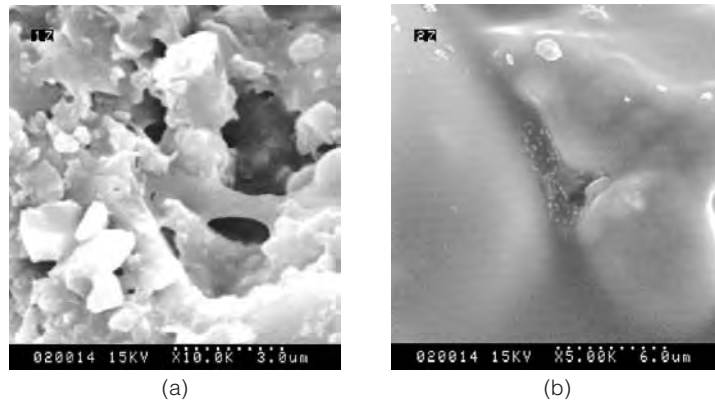
SEM Analysis. SEM was used to evaluate the consolidants. SEM micrographs of samples treated with the different consolidants were obtained. SEM images for samples treated with 20 percent F4-SS show the sandstone grains coated with a homogeneous smooth film (figs. 7a, b). Sandstone grains in the samples treated with WD-02 and Remmers 300 are not coated with the consolidant; instead, the network structure of the polymer gel has spread over the grain surfaces. SEM images of the sample treated with a mixture of F4-SS + 10 percent WD-10 just formed a very thin layer on the sample surface, leaving the quartz grain boundaries visible, and failed to fill fine cracks; therefore they were excluded from further tests.

SEM was used to study the penetration of the different consolidants. The low-viscosity consolidants of F4-SS showed good penetration. SEM also confirmed the failure of 30 percent F4-SS to penetrate the internal structure of the stone, either by capillary absorption or by total immersion absorption. This is due to its high viscosity and its fast polymerization. This is also the reason for the decreased porosity and water absorption values of samples treated with this consolidant.

SEM examination also showed that the macro pores are open when treated with a low concentration of F4-SS, permitting air movement inside the stone. This also makes it possible for salts to effloresce on the surface in situations when salts exist inside the structure of the stone. SEM images of H$_2$SO$_4$ erosion on samples treated by F4-SS revealed that only a few holes on the sample surface were formed after erosion; H$_2$SO$_4$ did not destroy the film.

FIGURE 7 SEM image of sample treated with 20 percent F4-SS showing (a) network and (b) sandstone grains coated with a homogeneous smooth film. 60,000× magnification.

(a)

(b)

In Situ Consolidation Demonstration

The effectiveness of the different consolidants was tested during an in situ demonstration in a cave at Zhongshan Grotto where the figures have been entirely lost. The demonstration was conducted during winter, and after one year of treatment in situ (2002), the treated sections were tested and evaluated. Because of the limited demonstration area provided, just four consolidants were used for the treatment: 20 percent F4-SS, 5 percent F4-SS, WD-02, and Remmers 300.

A 0.4-square-meter demonstration area was selected on the west side of the cave about 2 meters above the ground. This area was divided into four test sections, each to be separately treated by 20 percent F4-SS, 5 percent F4-SS, WD-02, and Remmers 300. Each section measured 720 square centimeters, with a 200-square-centimeter space left between adjacent sections.

Dust and surface efflorescence were first brushed off the test sections. Then the consolidants were applied at 0.57 to 0.8 kilogram per square meter. After one year, the four treated sections were tested for color variation, water absorp-

tion (by Kust-tube measurement), and drilling resistance. Results are given in table 6.

Figure 8 shows that the different consolidants perform similarly with respect to water absorption, with the exception of WD-02 in water uptake. The figure also shows that water absorption is continuous, without a turning point, which suggests also that the consolidation treatment is uniform from grotto surface to the interior. Because of exceptionally heavy precipitation in 2002, the test results should over time reflect the influence of water on the materials used.

Conclusion

Preliminary results from the yearlong in situ consolidant demonstration show that 5 percent F4-SS and 20 percent F4-SS, due to their low viscosity (similar to that of water), successfully penetrated the test sections and bound the friable sandstone grains into a hard structure.

F4-SS, a multifunctional polymer, contains a long alkyl chain; and because of its fluorine atoms, it has excellent anti-aging properties and water repellency. It contains hydroxyl

Table 6   Consolidant Demonstration Test Results

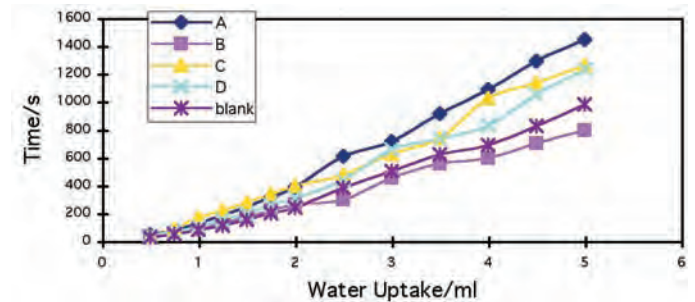| Test Section	Consolidant	Color Change (ΔE)	Water Uptake / $s \cdot ml^{-1}$	Drilling Resistance ($\Theta/10$)
A	Remmers 300	2.01	322.6	14.6
B	WD-02	1.73	173.7	12.6
C	20% F4-SS	2.98	273.3	13.4
D	5% F4-SS	1.85	265.6	14.4
Untreated	—	—	214.6	11.8–15.4

FIGURE 8 Water uptake for test areas A–D of in situ consolidant demonstration.

and acidic groups, which provide bonding to the stone surface. Therefore, fluorinated polymers can form a uniform film on the surface of the sandstone's mineral grains and bind them together, as well as fill in pores, which enhances the strength of stone. In the case of highly deteriorated stone, where a strong binding agent is needed to hold the grains together, it is possible to apply a higher concentration of fluorinated polymer. But no more than 30 percent should be used because of the high viscosity, decreased penetration, and rapid polymerization on the stone surface.

Accelerated weathering tests indicate that the fluorinated polymers provide treated stone with a longer life span, a stronger waterproof capacity, and increased resistance to acid. Thus fluorinated polymers should prevent stone from being attacked by acid water or rain. Because treatment with fluorinated polymers does not obviously influence porosity or water vapor permeability of the stone, these consolidants should be effective in reducing weathering. The treatment does not block the pores of the stone, so it should be possible to retreat stone successfully.

Notes

1   Remmers 300 was obtained from the Remmers Company, Germany. WD-02 is an alkyltrimethoxysilane, $C_{10}H_{21}Si(OCH_3)_3$, obtained from Wuhan University, tel. 027-87215023, 87214371, e-mail: sale@wdsilicone.cn. The mixtures of F4-SS + WD-10 were obtained from Wuhan University, Hubei province, China.

References

Alessandrini, G., L. Toniolo, and C. Colombo. 2000. Partially fluorinated acrylic copolymers as coatings for calcareous stone materials. In *Tradition and Innovation: Advances in Conservation: Contributions to the Melbourne Congress, 10–14 October 2000,* ed. A. Roy and P. Smith, 1–6. London: International Institute for Conservation of Historic and Artistic Works.

ASTM. 1997. *Standard Test Methods for Sampling and Testing Brick and Structural Clay Tile.* ASTM C67-97.

Ciardelli, F., M. Aglietto, V. Castelvetro, O. Chiantore, and L. Toniolo. 2000. Structurally modulated fluoropolymers for conservation of monument stones: Synthesis, stability and applications. In *Proceedings of the New Millennium International Forum on Conservation of Cultural Property, 5–8th December 2000, Deajeon, South Korea,* ed. Suckwon Choi and Mancheol Suh, 166–81. Kongju, Korea: Institute of Conservation Science for Cultural Heritage, Kongju National University.

He Ling and Liang Guozheng. 2003. Fluorinated membrane polymers as coatings for the conservation of culture properties. *Mo ke xue yu ji shu = Membrane Science and Technology* 23 (3): 40–45.

Mclain, S. J., B. B. Sauer, and L. E. Firment. 1996. Surface properties and metathesis synthesis of block copolymers including perfluoroalkyl-ended polyethylenes. *Macromolecules* 29 (25): 8211–19.

Nonaqueous Dispersions and Their Antiweathering Performance for Earthen Buildings, Monuments, and Archaeological Sites

Zhou Shuanglin, Yuan Sixun, Guo Baofa, and Xia Yin

Abstract: Commercially available aqueous dispersions of acrylic and silicon polymers were transformed into nonaqueous dispersions in organic solvents and after laboratory testing and evaluation on loess earth have been applied in limited though quite large areas at a number of Chinese archaeological sites, including the Terracotta Warriors (pit 1), the Neolithic site of Niuheliang, and the Fayuan Temple in Beijing. Results are positive.

Natural weathering is important in the deterioration of earthen archaeological sites and constructions. In China many archaeological sites, for example, Banpo in Shaanxi and Dahecun in Henan, are sheltered by buildings and are part of site museums. However, there are other sites left in the open air. Many of the latter show signs of deterioration, such as salt efflorescence and biological growth. To prevent these sites from weathering, many methods, such as surface consolidants and drainage, have been used.

Chemicals typically used as antiweathering agents are silicons, acrylics, polyurethanes, and organic latexes. These are effective in preserving earthen constructions from weathering, but each has disadvantages. Clay samples treated by acrylics show a change in color and disintegrate during water immersion tests; those treated with polyurethane also have a distinct color change, though they are resistant to water; treatment with tetraethoxysilane results in brittleness and poor freeze-thaw resistance; and silicons also show color change.

In order to choose a suitable chemical for preservation of exposed earthen constructions, we tested a number of chemicals. Acrylic latex showed good consolidation, and clay samples treated with low-solid-content acrylic latex had little

or no color change and were stable in water and freeze-thaw tests. The disadvantage was that the test samples disintegrated during treatment because of the high water content in the latex.

The question, then, was how to overcome the disadvantage of aqueous acrylic latex. Could we exchange water for organic solvents? Nonaqueous systems for the latex seemed to offer the best alternative. A nonaqueous dispersion consists of high molecular polymer particles (diameter 0.01~30 µm) dispersed in organic solvents. The polymer is not dissolved in the solvent but is dispersed in it, similar to a colloidal suspension. Two methods were used to produce nonaqueous dispersions:

- Polymerization: Monomers were polymerized in nonaqueous solvents by dispersion polymerization, which has been discussed in related patents (Walbridge 1973).
- Transfer: When organic solvent with surfactant is added to aqueous organic latex, the latex becomes unstable and agglomerates from the water phase, and transfer of polymer particles to the organic phase occurs, resulting in a nonaqueous dispersion. This method was first developed during the period 1970–80 (for patents, see Campion and Yardly 1971; Keown 1973). The transfer method is generally easier than polymerization, and the nonaqueous dispersion formed has a high solid content and low viscosity.

After many years of development, polymer latexes synthesized by emulsion polymerization have generated a vari-

ety of products for different requirements. Room temperature self-cross-linking acrylic latex and silicon-modified acrylic latex are categories of polymers that provide outstanding performance; the former leads the latex to form an organic film with different glass transition temperature (T_g) based on the latex composition and has good antiaging properties; the latter has better long-term stability than the former due to the silicon group. In this study several new species of room temperature self-cross-linking acrylic latexes and silicon-modified acrylic latexes were transferred to nonaqueous dispersions for testing and application.

Latexes

Acrylic Latex

- BA-154, BC-2021, and BC-4431, produced by Dongfang Chemical Plant, Beijing (table 1)

Silicon-Modified Acrylic Latex

- BC-251M, produced by Dongfang Chemical Plant, Beijing
- KX 2002, produced by Kexin Chemical Co., Beijing
- TD-1, produced by Sunrise Chemical Co., Jiangsu

All the latexes listed above were transformed into nonaqueous dispersions by the transfer method. The organic solvents used to disperse the polymer particles were cyclohexane, hexane, methylethyl ketone, cyclohexanone, and alcohol. The

nonaqueous dispersions transferred from BA-154, BC-2021, and BC-4431 are labeled 54J, 21J, and 31J, respectively.

Properties of the Dispersions

The properties of the latexes and acrylic nonaqueous dispersions and the film formed after the evaporation of the dispersants are presented in table 2.

Particle Size

Particle size was determined by transmission electron microscopy (TEM) after dilution to 1 percent and drying on a copper film at −25°C. Contrast was improved by dyeing with mercurochrome.

Viscosity

An Ubbelohde viscosimeter was used to determine the viscosity of 1~15 percent dispersions in cyclohexanone (table 3). Viscosity of acrylic nonaqueous dispersion increases rapidly with concentration. Silicon-modified acrylic nonaqueous dispersions show similar behavior.

Stability

High-solid-content (<15%) nonaqueous dispersions stored at room temperature for one year are stable and could be used

Table 2   Radius Determined by TEM

		Radius of Particles (mm)
	BC-4431	50
Latexes	BC-2021	100
	BA-154	150~400
Nonaqueous dispersions	31J	50
	21J	75
	54J	—

Table 3   Viscosity of Three Nonaqueous Dispersions at 25°C

Sample	(mPa)				
	1%	3%	7%	11%	15%
31J	3.35	6.52	17.0	38.0	66.2
21J	3.82	5.96	8.75	21.0	39.1
54J	2.74	3.63	10.2	85.9	

Table 1   Properties of Acrylic Latexes

Sample	Appearance	Solid Content	pH	MFFT°C	T_g
BC-4431	White liquid	41 ± 1%	6.5~7.7		41°C
BC-2021	White liquid	50 ± 1%	7~9	18°C	20°C
BA-154	White liquid	60 ± 1%	3.5~5		0°C

	Viscosity (mPa)	Composition
BC-4431	350~1500	Copolymer of styrene and ethyl acrylate
BC-2021	<500	Copolymer of acrylate monomers
BA-154	100~550	Copolymer of acrylate and a functional group

to consolidate loess samples with the same result as with freshly prepared dispersions.

Properties of Films

Films formed by evaporation of the dispersant are transparent to opaque, with different hardnesses, some soft and some hard. Photo-aging and heat-aging tests on the films showed excellent antiweathering resistance, especially for silicon-modified nonaqueous dispersions.

Consolidation Results

Consolidation properties of the nonaqueous dispersions were tested in the laboratory.

Nonaqueous Dispersion and Clay Samples

The porosity of the loess soil of China is between 40 percent and 53.1 percent. Loess excavated from Changping, Beijing, was crushed and screened, then mixed with water to 9.5 percent by weight water content. The mixture with weights of 310 grams and 270 grams was molded into 50- by 100-millimeter columns with porosity of 41.1 percent and 48.8 percent, corresponding to the upper and lower limits of porosity of this loess.

The solid content of nonaqueous dispersions used to consolidate the loess columns was between 1 percent and 7 percent (table 4). Dispersions with solid content between 0.5 percent and 3 percent showed the best consolidation performance.

Loess samples were saturated with consolidant by capillary rise. Each loess column absorbed 80 to 100 milliliters of nonaqueous dispersion. To fulfill systematic test requirements, 18 columns were made for each kind of dispersion at the same solid content. After two to seven days of evaporation of solvent, saturated loess columns became hard and stable. These were used for testing the consolidation ability of nonaqueous dispersions.

Test Methods and Results

Weight Change. Loess columns consolidated by nonaqueous <3 percent solid content dispersions showed a weight gain of 3 grams or less.

Color Change. Usually the color change was so minimal that it could not be perceived by the naked eye.

Permeability. Permeability of loess consolidated (31J, 21J, and 54J at 1, 2, and 5 percent concentration) samples as determined by immersion in water. It was found that consolidation did not significantly affect permeability.

Rupture Strength. The rupture strength of loess columns consolidated by 31J, 21J, and 54J was determined (table 5).

Water Resistance. Loess columns (270 g) consolidated with 31J, 21J, and 54J (solid content greater than 1 percent) were stable in water without cracking or disaggregation, except for columns consolidated with 21J, more than 5 percent of which failed.

Freeze-Thaw Tests. Freeze-thaw tests (4 hours of immersion in water and 4 hours at −25°C) were conducted. Loess columns consolidated by 31J cracked in the first freeze-thaw cycle, and the crack opened in the next cycles; some columns broke into pieces. Loess columns consolidated by 21J showed good results, except for one column in which particles fell from the surface. Loess columns consolidated with 54J showed good results, except for several in which small cracks appeared.

Salt Resistance Tests. Consolidated loess columns were dipped into 5 percent sodium sulfate solution for 8 hours, then dried at 100°C for 4 hours to complete one cycle. Loess consolidated with 31J cracked and broke into pieces after

Table 4   Consolidants Used and Their Applied Concentrations

Solid Content	
310 g	**270 g**
1%, 3%	1%, 3%, 5%, 7%
1%	1%, 3%, 5%
1%	1%, 3%, 5%, 7%

Table 5   Rupture Strength of Treated Clay Samples

Solid Content (%)		Rupture Strength (kg)		
		31J	**21J**	**54J**
310 g	0	170	170	170
	1	200	220	316
	3	320	296	
270 g	0	47	47	47
	1	50	70	50
	3	68	100	97
	5	101	137	
	7	127		

FIGURE 1 Consolidation of the dividing wall in pit 1 of the Terracotta Warriors. The front wall is untreated; the rear wall is treated.

three cycles. Loess consolidated with 21J gave a good result, although the sample with solid content of 3 percent developed small cracks after three cycles. Loess consolidated with 54J also developed cracks and the upper part was destroyed after the cycles.

Application Testing on Archaeological Sites

The Terracotta Warriors Site

Small-scale tests of the consolidation effectiveness of nonaqueous dispersions were conducted at several locations at the site of the Terracotta Warriors of the first emperor of the Qin dynasty. Because the results were good, a middle-scale test was conducted on a dividing wall, 15 by 18 by 1.6 meters (length × width × height) in pit 1. The surface area was about 45 square meters. 31J consolidant at 2.5 percent concentration was used. Consolidant was sprayed on the vertical surface of the dividing wall repeatedly until the soil was saturated. After application, the area was covered by plastic film for one week in order to avoid rapid evaporation of the solvent. Penetration was about 4 centimeters. The consolidated surface was periodically inspected over three years. The result was good (fig. 1): the surface had little or no color change, and it was so hard that no loss of earth occurred when scratched.

The Yang Mausoleum

The Yang Mausoleum of Emperor Jing (r. 188–144 b.c.e.) of the Western Han is located in Xianyang City, Shaanxi province. The test was done on a wall of the tomb and a wall of the ramp where an imprint of a decayed wooden member occurred. Each area was 60 by 70 centimers and required 6 and 5 liters, respectively, of 31J at 2 percent concentration. The result was examined after five months and again after two years. The tomb surface was hard but had some color change (fig. 2). The wood imprint was hard; however, the unconsolidated areas showed signs of weathering.

Niuheliang

Niuheliang is a Neolithic Hongshan culture (5000–3000 b.c.e.) site of national significance, discovered in 1981 in Liaoning province. The site has been heavily weathered after excavation. After consolidation testing in the laboratory, two nonaqueous dispersions were used on small (50 by 50 cm) areas. 31J (2% concentration) and 251M (1% concentration) were applied to the top and side surfaces of a dividing wall (an unexcavated earth body). The treated areas were then covered by plastic film so as to minimize the loss of solvent due to wind, which could affect the consolidation. A month later, a depth of penetration of 12 centimeters on the top of the dividing wall and a depth of 8 centimeters on the side of the same wall were achieved with 31J, and a depth of 8 centimeters was achieved on a side wall of 251M.

FIGURE 2 Consolidation of the wall of the Yang Mausoleum. The left side is untreated; the right side is treated.

The Fayuan Temple

The Fayuan temple was built in the late seventh century in present-day Beijing and renovated several times in its history. During restoration work in 2002, rammed earth walls were found in the bell and drum towers of the temple. The decision was made to preserve the walls in the traditional manner, by attaching hemp fiber and then coating them with lime plaster. But it was found that the walls were too weathered to hold the hemp fiber and lime plaster. After testing on small samples, 31J (1.2–1.5% concentration) was applied to the weathered areas. After three days, the treated surfaces were stabilized, and hemp fiber and lime plaster were applied to them.

Conclusion

Nonaqueous dispersions have proved superior to water-based acrylic latexes in several respects. Our laboratory tests showed that they cause insignificant weight and color changes and produce positive results in consolidating soil samples, which were confirmed by field tests.

References

Campion, R. P., and J. F. Yardly. 1971. Manufacture of polymeric compositions. U.S. Patent 3574161 filed February 28, 1968, and issued April 6, 1971.

Keown, R. W., inventor. 1973. Manufacture of solutions and dispersions of polymers in organic liquids from a polymer latex. U.S. Patent 3733294 filed November 25, 1970, and issued May 15, 1973.

Walbridge, D. J., inventor. 1973. Polymer dispersions. British Patent 1305715 filed July 4, 1973, and issued February 7, 1973.

Consolidation Methods for Cracks at the Qin Terracotta Army Earthen Site

Zhang Zhijun

Abstract: *After archaeological excavation of the Terracotta Warrior burial pits, the rammed earth walls dried out and developed large structural cracks. This paper reports on stabilization techniques, including the use of steel braces, plates, and rods, and also continued treatments with potassium silicate consolidate. After evaluation the recommended treatment was determined to be rock bolts of sand and lime with propping of cracked walls with steel plates.*

In the Qin Mausoleum of the First Emperor, auxiliary burial pits 1, 2, and 3 are large-scale underground structures made of earth and timber. The side and dividing walls of the pits are built of layers of rammed earth, each layer with an average thickness of 10 centimeters. These earthen structures are an integral part of the main burial pit and have important cultural significance.

Some parts of the side and dividing walls had already collapsed before excavation, due to periodic flooding over the centuries. The weight of the 2 to 3 meters of topsoil exerted pressure on the underlying structures. After excavation the environmental conditions changed and led to rapid loss of moisture. Consequently, lateral stress relief resulted in fissures up to 10 centimeters wide in the side earthen walls and partitions. A number of long cracks parallel to the side and dividing walls developed, threatening collapse. This situation threatened the site and the terracotta figures between the partition walls (fig. 1). In order to preserve this important heritage site, extensive experimental research on preservation of the earthen structures was carried out.
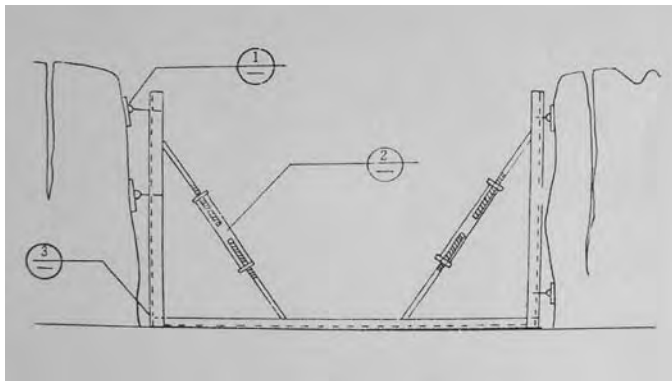
Consolidation Methods

Five consolidation methods were tried, as follows.

U- and H-Shaped Steel Reinforcement Supports
In 1988 some parts of a dividing wall were about to collapse. U- and H-shaped steel was used to stabilize ten areas of fissuring (figs. 2, 3). The steel was treated with anticorrosion material, and after installation the supports were further treated to blend visually with the earth.

FIGURE 1 Ten-centimeter-wide cracks on the earthen partition wall in pit 1.
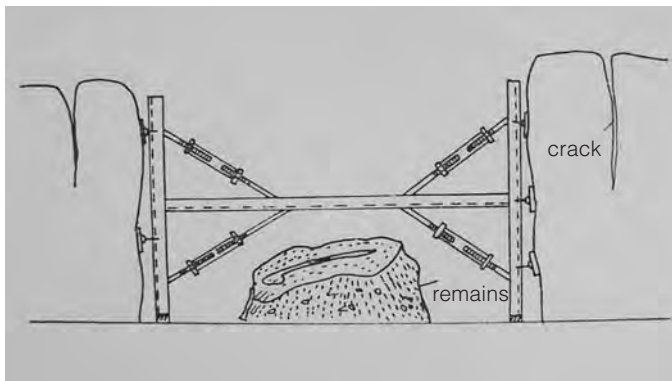
(a)

FIGURE 2 U-shaped bracket for reinforcing the earthen partition wall.

(b)

(a)

FIGURE 3 H-shaped bracket for reinforcing the earthen partition wall.

(b)

Wall Stabilization with Steel Plates

In 1991 an additional measure was taken to stabilize the walls. Steel plates on both sides of a wall were secured with a steel bar through the wall and anchored into the ground with cement (fig. 4). Cracks were filled with earth to improve the visual effect (fig. 5). The method was used in parts of pits 1 and 3 instead of the U- and H-shaped steel supports.

Steel Rod Grids

Two large cracks developed on the overhang of the entrance-way to the east wall of pit 1. The cracks ran from the top to the bottom of the wall, and a huge mass of earth was in danger of collapsing. Steel rods were embedded into grooves cut into the earth structure. The rods were tied together with bars penetrating the walls to create a grid. The whole was secured to the ground with cement.

Combined Physical and Chemical Consolidation

Combined physical and chemical consolidation was tested by Li Zuixiong and Wang Xudong of the Dunhuang Academy in 1996. A relatively thin fracture on the northern wall of pit 1 was filled with potassium silicate slurry and anchored with specially made anchor rod and slurry.

Anchor Bolts with Sand and Lime

From 1999 to 2001 a joint Sino-German project used aluminum rock bolts with sand and lime for consolidation of two areas of endangered dividing walls of pits 1 and 2. The equipment, designed especially for the project, was capable of both boring and filling the sand and lime in the holes (fig. 6). The anchor rod was aluminum alloy of 8 millimeters diameter. The mixture was made of 90 percent fine sand (water washed and passed through a 1 mm screen), 5 percent
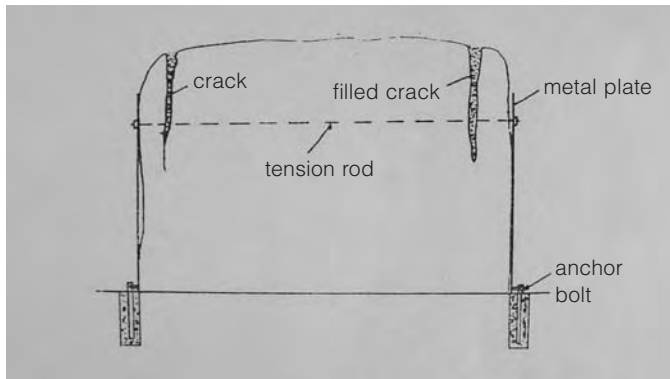
FIGURE 4 Steel plates for reinforcing the earthen partition wall.

FIGURE 5 Condition of the earthen partition wall after use of steel plates for reinforcing. The imprint of steel plates can be seen on the wall.

cement, and 5 percent white lime. The slurry was made with deionized water.

Evaluation of Methods

U- and H-shaped steel supports were effective in preventing collapse but left evident changes in the appearance and also impeded the restoration work of putting the terracotta figures back into their original positions. This method can be justified only when the need is urgent; in general, it is unacceptable for future conservation of the Terracotta Army.

Use of steel plates has the advantages of being a simple, safe technique and of being reliable and durable. It is a useful method for consolidating the dividing walls, especially when cracks occur on both sides of a wall. But it has drawbacks. Boring through the wall often damages its other side because of the pressure exerted. It is also difficult to drill holes from both sides that will meet each other, since the walls are thick. In addition, securing the system to the ground with cement bricks requires the removal of the original floor bricks.

The steel grid used for the eastern wall of pit 1 also had drawbacks: it damaged the wall surface and affected the appearance. Although this method prevented collapse of huge structural parts, other considerations need to be taken into account for future applications. If it were integrated with a restored wooden structure, as was present originally, such that the appearance was not affected, it could be used.

The combined physical and chemical treatment was satisfactory as an experiment, but the method is difficult to use and to control. The potassium silicate slurry is water based and the shrinkage on drying rather large. This would be likely to cause new cracks. In addition, use of water weakens the earthen structure and adds to the risk of collapse. Therefore, we do not recommend this method, especially as simpler solutions to the problem exist.

Anchor bolts with sand and lime proved most satisfactory. The technique has the advantages of high efficiency, excellent appearance, low cost, and reliability, and it can be used in dry and wet situations. Compared to the other stabilization methods, in general, it is the best way to conserve the Terracotta Army pits.

FIGURE 6 Reinforcing with the anchor bolts and grouting method.

Conclusion

Because of the complexity of the existing conditions of the site, more than one type of conservation is required, even when one method is considered the best. We propose the following options for the site: rock anchors with sand and lime, propping up both sides of a wall with steel plates, and improved steel grid frames. The final decision has to be based on the location and condition of the cracks. The U- and H-shaped steel supports, the combined physical and chemical consolidation method, and the unimproved steel mesh frames should no longer be used.

The Conservation Program for the Castle Ruins of the Guge Kingdom in Ali, Tibet

Wang Hui

Abstract: *The Guge Kingdom was one of the regional regimes established in the ninth century by the descendants of the Tibetan Empire in the Ali area in western Tibet. The main castle, which was the center of the kingdom, was located on a hill in Zhaburang (currently Zhada county). The area was abandoned when the regime collapsed in the seventeenth century. Today the site consists of ruins of residences, temples, grottoes, and defensive structures, which occupy an area of nearly 720,000 square meters. From 1996 to 1999 the State Administration of Cultural Heritage provided funding for a conservation project. Conservation technicians from Hebei and Shaanxi provinces and other areas joined the Cultural Heritage Bureau of the Tibet Autonomous Government to implement the conservation project at the site. The author participated in the project for its duration and was in charge of the project's investigation and design. This paper focuses on the working process and technical solutions.*

From 1996 to 1999 China's State Administration of Cultural Heritage (SACH) funded a program to conserve the weathered and endangered cultural heritage sites in Ali, a remote and distinguished region in Tibet. The central government considered this effort a key program to aid the Tibet Autonomous Region. Three main sites were involved: the castle ruins of the Guge Kingdom, the Tuolin Monastery, and the Dongga Piyang Ruins, all of which are on the list of China's designated historic sites. The program, with a total expenditure of more than 10 million RMB (Wang Hui and Pengcuolangjie 2002), was the largest comprehensive conservation effort in Tibet aside from the conservation program of the Potala Palace. The program, which involved not only architectural conservation but also archaeological research,

engaged experts and technicians of diverse ethnic groups from Tibet, Hebei province, Shaanxi province, and Beijing.

This paper discusses the conservation effort for the castle ruins of the Guge Kingdom. The site is located on a hill in the far western section of the Qing-Zang plateau, in a basin between the Himalaya and Gangdise mountain ranges, adjacent to India and Kashmir. Next to the hill the river Langqinzangbu (Xiangquanhe) flows to the north. The altitude of the site is between 3,680 and 3,800 meters above sea level.

History of the Guge Kingdom's Castle Ruins

The historic kingdom of Guge can be traced to the ninth century C.E., following the collapse of the Tubo dynasty. When the king of Tibet was assassinated by a lama in 842, one of his descendants, Jidenimagun, fled to Zhaburang, in the western part of Ali, and was empowered by the local authorities. He married the daughter of the indigenous king and developed the region into a strong realm in western Tibet. After Jidenimagun passed his power to his three sons, the realm was divided into three parts, one of which was called the Guge Kingdom, which occupied the Zhaburang region. The king of Guge and all his successors believed in and promoted Buddhism, and as a result many monasteries were built in the region, near the capital. Among them, Tuolin Monastery was the most prestigious. One of the kings invited an Indian monk, Master Atisa, to reside in the monastery (Su Bai 1996). Because of Tuolin Monastery, Guge became one of the two cradles of the Tibetan Buddhist movement. In the second half of the seventeenth century, weakened by conflicts between different religious groups, Guge was invaded and occupied by the neighboring

389

FIGURE 1 Guge Kingdom site view.

FIGURE 2 Mountaintop ruin.

kingdom of Ladak. The Guge Kingdom, which had lasted for about eight centuries, came to an end.

The Guge Kingdom's castle was a large complex of buildings that housed the central administration. After the kingdom's collapse, the site was abandoned. The castle ruins cover a 720,000-square-meter area that is 600 meters long east-west and 1,200 meters wide south-north. Major buildings were terraced along the eastern slope of the hill. More than 400 temple buildings, nearly 1,000 grottoes, 58 defense towers, 4 secret passages, 28 pagodas, 11 warehouses, and various accessory houses were documented. All the buildings were made of earth and timber. Currently, only five temple halls are structurally intact; other buildings have either collapsed completely or are partially standing, with only the deteriorated walls extant. Owing to the region's arid climate and the desolate location, the original state of the ruins was preserved (figs. 1, 2) (Xizang gong ye jian zhu kan ce she ji yuan bian 1988).

The earliest on-site survey of the castle ruins was conducted during the 1920s and 1930s by Giuseppe Tucci, a scholar who worked in the Oriental Institute in Italy. In 1961 the State Council designated the Guge Kingdom's castle ruins a historic site of national significance. Beginning in the 1970s, a professional survey of the site was organized.

Planning and Implementing the Castle Ruins Conservation Project

The author was in charge of the investigation and design phases of the project, as chief engineer. Based on the sugges-

tions of experts after their preliminary inspection of the site in 1996, the project team worked out a scientific and orderly procedure and methodology to follow during the conservation process, as follows:

- Staff. The staff comprised architects, engineers, conservators, archaeologists, geographers, and scholars of Tibetan studies. Team members were from different ethnic groups, such as Tibetan, Muslim, and Han. Four professional groups comprising engineering, archaeology, documentation, and liaison were organized, and all tasks were assigned.
- Data collection. This included historical, climatic, geologic, and archaeological information, as well as records or documentation on historical interventions and existing publications.
- Survey. A detailed on-site survey and assessment was conducted, which included recording measurements and mapping and visiting similar sites in the vicinity for reference.
- Applicable technology. Local traditional construction skills, as well as the possibility of applying new technology in the project, were reviewed. Advice and suggestions were solicited from local technicians and monks.
- Final conservation plan. The final conservation plan was drafted and forwarded to Tibetan cultural heritage officials and then to SACH.
- Plan evaluation. Seminars were organized for experts to evaluate the plan for approval.

- Investigation. Archaeological investigation of relevant sites was conducted before any work was undertaken.
- Implementation. Project tendering and implementation of the conservation plan were undertaken, with on-site supervision of the contractor.
- Approvals. Regular checks were made of each project component before the completed work was approved; SACH gave final general approval to the project.
- Maintenance plan. A maintenance plan, including a detailed work schedule, for the site was written. Financial resources were budgeted to carry out the maintenance.
- Project reports. A project summary was prepared, and conservation reports were compiled and edited.

On-Site Survey and Assessment

The hill on which the castle ruins are located is bare of any vegetation, and the geology is of the Quaternary period. The rock is easily cut and eroded by water. Ruined walls were made of either rammed earth or earthen blocks that erode easily. Occasional heavy rainfall (occurring once or twice every July and August, with an average annual rainfall of less than 100 mm) and frequent strong winds are the dominant elements that damage both the hill and the buildings. Other factors, such as uncontrolled accessibility to tourists and local people, also threaten the site.

The main problems at the site relate to water: erosion, cracked and leaning walls, collapsed roofs, and deterioration of walls and indeed of the entire topography required emergency consideration (fig. 3). This paper does not deal with the grottoes and their paintings. It can be noted, however, that extensive damage arising from the loading of buildings above the grottoes with deformation of the cave walls occurred. In many cases, stagnant water accumulated in the decorated caves. In some cases accumulation of soil due to collapsed entrances tended to direct water into the cave interior.

In fact, poor drainage undermines the entire site. As mentioned, the rains are of short duration but heavy. This type of precipitation is especially damaging to urban structures. Originally, the complex had an effective drainage system, and some water outlets are still functioning. After abandonment, debris started to block outlets and resulted in progressive erosion within the ruins.

Conservation of the Castle Ruins

The walls that remain standing on the site of the Guge castle are uniquely picturesque and embody the history and evolution of the castle complex (fig. 4). Therefore, maintaining the ruins in their present condition was important. Eliminating all causes of damage was unrealistic. We worked out a practical conservation plan that emphasized reinforcing at-risk sections and improving stability of especially important parts of the ruins. Repair and reinstatement of the drainage system to reduce the effects of water were key interventions. The final goal of the conservation project was to minimize deterioration and preserve the ruins as a whole.

The philosophy and principles guiding the design and implementation of the conservation effort were based on the heritage conservation law of China and relevant national charters and recommendations. The following points were key:

- Consolidation and engineering interventions were kept to a minimum. The visual effects of interventions were as inconspicuous as possible, and all additions were compatible with the fabric of the site.

FIGURE 3 Cracking and threatened collapse of earthen architecture.

FIGURE 4 Building foundations and the mountainside eroded by rainwater.

- The interventions had to be reversible. Since most parts of the site were not excavated, it was necessary to minimize the disturbance of debris and deposits to preserve the site as far as possible.
- Local materials and the traditional skills of the local population were employed to the extent possible.

Project Details

Specific work to conserve the castle ruins is described below.

1. Standing walls:
   - Severely deteriorated blocks or lost parts were replaced.
   - Earthen walls suffering from vertical cracks were capped and wood lintel timbers inserted to bridge vertical flaws.
   - Leaning walls were buttressed, and rubble was inserted at the base of the buttresses to protect the earthen walls from erosion.
   - Caves with structural cracks were stabilized with support columns painted black to blend in with the surroundings.
   - Missing roof slates were replaced.

2. Upgrading to alter and control water drainage:
   - Decreasing the water retention time on the site and flow distance and allowing water to escape as

quickly as possible were key factors. Retrofitting water outlets was achieved by reducing the number of outlets at the edge of the hill and consolidating large outlets with erosion-resistant materials (fig. 5).
   - The topography of the site was modified by partial filling and excavation to reduce water pooling.
   - Dikes or ditches were constructed along sensitive areas to control the water flow direction and to avoid water flow to architectural ruins.
   - Small water outlets were blocked with rubble and mortar to direct water to larger outlets.
   - Timber roofs were added, and holes were filled with clay to exclude water.
   - Large flat areas were paved and drained.
   - Pipes were added to the site to remove water.

3. Roofs: New roofs in the Tibetan style were added to extant buildings to prevent rainfall from affecting wall paintings and entering lower caves. The appearance of these roofs is consistent with the site's setting. Damaged roofs were restored in accordance with evidence discovered from investigation or archaeological work (fig. 6).

4. Intact halls: Intact halls, such as the White Hall, the Red Hall, and the Daweide Hall, were repaired in a simple fashion with little alteration. Tibetan
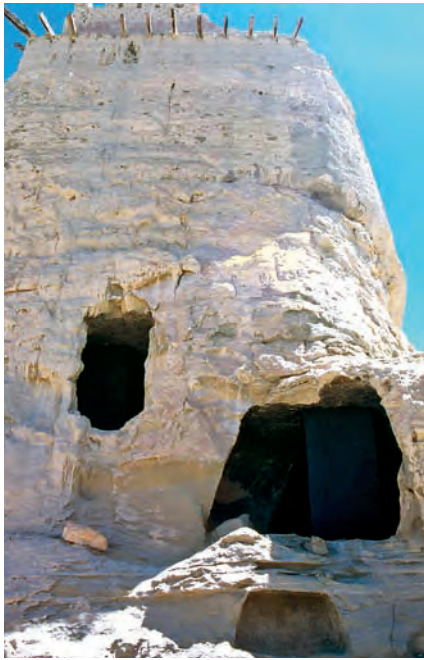

FIGURE 5 Drainage system.

FIGURE 6 Ruin stabilization and support.

architecture is distinguished by the use of Bianma straw decoration on the top of parapets. During conservation of the halls, some lost Bianma straw was reinstated and cracked rafters and decayed roof boards above rafters replaced, and clay was used to seal leaking roofs.

5. Other projects: A five-bay house in traditional Tibetan style was constructed near the site to accommodate the on-site custodians. A special pathway for visitors was paved with local slate. In addition, presentation and information were provided in some places on the site.

Conservation Results

In 1999, after years of arduous work, the project to conserve the castle ruins of the Guge Kingdom was successfully completed. The original character of the site and the sense of a desolate landscape were preserved, and minimum intervention was the underlying policy. Most important, dangerous conditions at the site were eliminated or mitigated. Meanwhile, new discoveries were made during archaeological work that filled gaps in the historical information on the site.

In June 1999, after three days of on-site evaluation and verification, the project was approved by an expert panel organized by SACH. The panel commented, "The original situation of the site and buildings were well respected during design and implementation. The critical causes of deterioration were restrained or eliminated on completion of the project. The expected aim and target were achieved through feasible and practical planning and careful construction" (SACH, PRC, and Ali Area 1999).

References

State Administration of Cultural Heritage (SACH), PRC, and Ali Area Cultural Heritage Emergency Intervention Project Team. 1999. Emergency intervention results assessment report on ruin sites, Tuolin Temple, Dongga Piyang site in Ali Area, Tibet. Archival document in Bureau of Cultural Relics, Tibet Autonomous Region, People's Republic of China.

Su Bai. 1996. *Zang chuan Fo jiao si yuan kao gu = Archaeological Studies on the Monasteries of Tibetan Buddhism.* Di 1 ban ed. Beijing: Wen wu chu ban she.

Wang Hui and Pengcuolangjie. 2002. *Xizang Ali Diqu wen wu qiang jiu bao hu gong cheng bao gao.* Beijing: Ke xue chu ban she.

Xizang gong ye jian zhu kan ce she ji yuan bian. 1988. *Guge wang guo jian zhu yi zhi.* Beijing: Zhongguo jian zhu gong ye chu ban she: Xin hua she dian Beijing fa xing suo fa xing.